Late Holocene paleosecular variation and relative paleointensity records from Lagoa dos Patos (southern Brazil)

Camila T. Lopes [a,*], Jairo F. Savian [b], Everton Frigo [b,c], Gabriel Endrizzi [b], Gelvam A. Hartmann [d], Nicolau O. Santos [e], Ricardo I.F. Trindade [f], Michel D. Ivanoff [a], Elirio E. Toldo Jr [b], Gerson Fauth [g], Lucas V. Oliveira [g], Marlone H.H. Bom [g]

[a] Programa de Pós-Graduação em Geociências, Universidade Federal do Rio Grande do Sul, Av. Bento Gonçalves, 9500, 91540-000, Porto Alegre, Brazil
[b] Instituto de Geociências, Universidade Federal do Rio Grande do Sul, Av. Bento Gonçalves, 9500, 91540-000 Porto Alegre, Brazil
[c] Universidade Federal do Pampa, Avenida Pedro Anunciação, 111, 96570-000, Caçapava do Sul, Rio Grande do Sul, Brazil
[d] Instituto de Geociências, Universidade Estadual de Campinas, Rua Carlos Gomes, 250, 13083-855, Campinas, SP, Brazil
[e] Instituto de Informática, Universidade Federal do Rio Grande do Sul, Av. Bento Gonçalves, 9500, 91509-900 Porto Alegre, Brazil
[f] Departamento de Geofísica, Instituto de Astronomia, Geofísica e Ciências Atmosféricas, Universidade de São Paulo, Rua do Matão, 1226, 05508-090, São Paulo, Brazil
[g] Instituto Tecnológico de Paleoceanografia e Mudanças Climáticas (itt Oceaneon), UNISINOS, Av. UNISINOS, 950, 93022-750 São Leopoldo, RS, Brazil

ARTICLE INFO

ABSTRACT

Lake and lagoon sediments are important recorders of the Earth's magnetic field variations. However, the Southern Hemisphere, particularly the South American continent, contributes only a small fraction of the global paleosecular variation (PSV) and relative paleointensity data, which hinders a better understanding of the global PSV. Moreover, the scarcity of information on the geomagnetic field in South Brazil for the past few millennia impedes, for example, a detailed analysis of the evolution of the South Atlantic Magnetic Anomaly (SAMA), which encompasses the weakest geomagnetic field on the Earth's surface. Here, we present high-resolution paleomagnetic and rock magnetic data of two cores collected at the lagoon of Lagoa dos Patos, Rio Grande do Sul State, Brazil. Sediment cores from Lagoa dos Patos represent the period from ~4540 to 3320 cal years BP. Rock magnetic results show the remanent magnetization resides in pseudo single-domain (PSD) magnetite and/ or titanomagnetite. Magnetization inclinations and declinations were isolated after alternating field demagnetization (AFD) and principal component analysis (PCA). Mean inclinations are −39,6° and − 38,4° for cores PT-04 and PT-06, respectively. Relative paleointensity results are compatible with geomagnetic field models, implying very promising results in the reconstruction of a reference curve for the region. As there is no PSV and relative paleointensity data for this region in this period, this study helps to elucidate the past field and the presence of SAMA in South America.

1. Introduction

Sediments are important archives to reconstruct the variability of the geomagnetic field beyond the historical period. This kind of record provides continuous geomagnetic field data, which allow constructing geomagnetic field models (Korte et al., 2009; Korte and Constable, 2011; Korte et al., 2011; Nilsson et al., 2014; Pavón Carrasco et al., 2014; Constable et al., 2016; Panovska et al., 2019). These models are used to better constrain the core field dynamics at decadal to millennial timescales (Dumberry and Finlay, 2007; Gallet et al., 2009; Amit et al., 2011;

Terra-Nova et al., 2015) and are useful on numerical dynamo simulations (Christensen et al., 2010). In addition, the geomagnetic field paleointensity models provide information to modulate the flux of cosmic particles (^{14}C, ^{10}Be), which are used to reconstruct the past solar activity (e.g., Suganuma et al., 2010, 2011; Muscheler et al., 2014). Finally, geomagnetic models and high resolution data for the past few millennia are used to understand important geomagnetic field structures, such as *archeomagnetic jerks* (Gallet et al., 2003, 2009; Snowball and Sandgren, 2004; Barletta et al., 2008; Yu et al., 2010) and the presence of a strong non-dipole field feature in the South Atlantic and

South America, called South Atlantic Magnetic Anomaly (SAMA) (Olson and Amit, 2006; Hartmann and Pacca, 2009; Hartmann et al., 2010, 2011, 2019; Terra-Nova et al., 2017; Trindade et al., 2018).

However, the spatial and temporal resolution of sediment records are fundamental for the accuracy of past field reconstructions (e.g., Donadini et al., 2009; Hellio and Gillet, 2018). High-resolution paleomagnetic sedimentary data records for the Holocene are unevenly distributed around the globe, being mainly concentrated in the Northern Hemisphere with little data in the Southern Hemisphere (Fig. 1a). This heterogeneity in data distribution directly influences the understanding of past geomagnetic field variations (e.g., Guyodo and Valet, 1996; Laj et al., 2004; Korte et al., 2005; Genevey et al., 2008; Korte and Constable, 2011). Scarcity and accessibility of basins with high sedimentation rates in the Southern Hemisphere are the most excellent significant limitations to obtaining high-resolution continuous records

for the Holocene (Fig. 1b). Furthermore, several studies have presented dating inconsistencies in the sedimentary database (Donadini et al., 2009; Korte et al., 2009; Nilsson et al., 2010; Korte and Constable, 2011). In addition, sedimentary records contain uncertainties in time and are inherently smoothed due to the post-depositional lock-in of magnetization (Roberts and Winklhofer, 2004). Declination and inclination data contain errors due to the difficulties in orientation of sediment cores (e.g., Snowball and Sandgren, 2004). There are also errors due to the sedimentary processes, such as compaction, which may lead to inclination shallowing (e.g., Tauxe, 1993). Despite these difficulties, considerable efforts have been made in the Southern hemisphere to obtain reliable paleomagnetic records for Quaternary ages (e.g., Brachfeld et al., 2000; Mazaud et al., 2002; Stoner et al., 2002, 2003; Gogorza et al., 2002, 2004, 2006, 2011, 2012, 2018; Kaiser et al., 2005; Macri et al., 2005; Macrì et al., 2010; Willmott et al., 2006; Irurzun et al.,
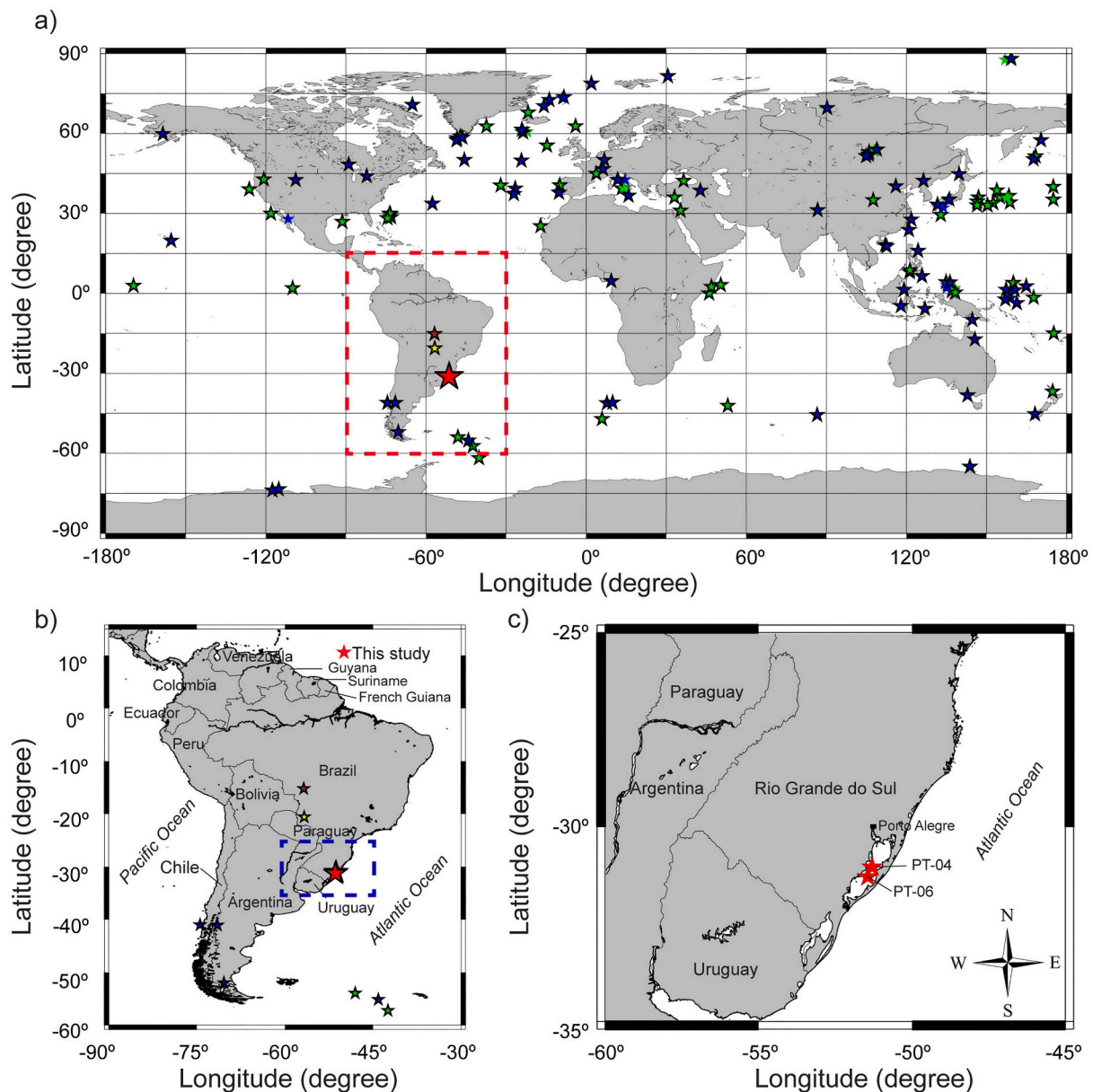

Fig. 1. Location of paleomagnetic sedimentary records for the Holocene: (a) around the globe, (b) in South America (data used in a) and b) are available in Panovska et al., 2018); (c) location of cores PT-04 and PT-06 in the Lagoa dos Patos lagoon. Red stars indicate the location of the two studied sites. Blue (green) stars indicate the location of sedimentary records that overlap (does not overlap) our new data. Brown star indicates the location of the stalagmites discussed by Trindade et al., 2018, and yellow star the location of the stalagmites discussed by Jaqueto et al., 2022. (For interpretation of the references to colour in this figure legend, the reader is referred to the web version of this article.)

2006; Lund et al., 2006; Nilsson et al., 2011; Hartmann et al., 2010, 2011, 2019; Collins et al., 2012; Lisé-Pronovost et al., 2013; Turner et al., 2015; Poletti et al., 2016; Channell et al., 2017; Trindade et al., 2018). One of the main purposes of this study is to report new paleomagnetic data from South Brazil for the Late Holocene to better constrain the past geomagnetic field variations in South America.

Here, we present the first results of the PATOS Drilling Project (PATOS), a research initiative to study the geomagnetic secular variation and environmental magnetism during the Holocene in South Brazil. The study site is located in the Lagoa dos Patos, considered the largest lagoonal system in South America (Fig. 1c). The recovery of sediment sequences from the Lagoa dos Patos lagoon enables us to obtain a geological archive to reconstruct the past millennial-scale variability of the geomagnetic field beyond historical time. The studied samples were obtained from two gravity cores (PT-04 and PT-06) collected in Lagoa dos Patos (Fig. 1c).

2. Geological settings and sedimentological studies

The Lagoa dos Patos is ~240 km long, ~40 km wide and average depth is almost 6 m. It covers an area ~ 10,000 km2, running roughly NE-SW direction, and is located in the coastal plain of Rio Grande do Sul State, South Brazil (Fig. 1c).The coastal plain is the southernmost area of Rio Grande do Sul and its East side is limited by the basement while the northern part is covered by Paleozoic and Mesozoic sedimentary and volcanic sequences of the Paraná basin. The northern part of the State has a relief with elevations that can reach 1000 m, while the southern relief is smoother, with altitudes that do not exceed 400 m. The Rio Grande do Sul coastal plain typically consists of unconsolidated Quaternary deposits, all related to transgressive events, which developed depositional systems, consisting of barriers and lagoons. The plain has an extensive number of lagoons and coastal lakes occupying almost one third of the coastal plain which has a surface of 33,000 km^2. Therefore, Lagoa dos Patos is a key site for high-resolution paleomagnetic and paleoenvironmental reconstruction at mid-latitude in the Southern Hemisphere.

The lagoon connects with the Atlantic Ocean through a single inlet - the Rio Grande Channel, at the southernmost part of the lagoon, where the mean tidal range equals to 0.31 m (Andrade et al.2018), and mean discharge of 4800 m^3/s. Sea water penetrates the lagoon up to 200 km to the north during exceptional conditions favored by southern winds, low water level in the lagoon, and spring tides (Martins et al., 1989; Toldo Jr., 1989). Previous studies suggest a continuous accumulation of sediments in the Lagoa dos Patos (Toldo Jr. et al., 2000; Toldo Jr. et al., 2006). According to these two works, the lagoon is a large and shallow coastal water body, protected from the waves of the nearby ocean. The lagoon receives freshwater from a drainage area of about 170,000 km^2, mostly from the Guaíba River System whose mouth, the Jacuí Delta, is at the city of Porto Alegre at the northwestern end of the lagoon (Fig. 1c). As a result, much of the lagoon has a salinity of less than3%. A much smaller contributor of freshwater to the lagoon is the Camaquã River. The combined watersheds of these two rivers cover almost half the area of the state of Rio Grande do Sul. The water in the Lagoa dos Patos has a residence time of about 108 days as estimated by Toldo Jr. et al. (2006). Whereas the Guaíba River contributes principally mud to the lagoon, the Camaquã River contributes principally sand. Sediments of the lagoon floor have <4% sand and consist mainly of silt and clayey silt in the northern half of the lagoon and silty clay in its southern half. Greenish gray colours predominate. Present-day deposition of muds occurs in water depths below normal wave base, which rarely exceeds 4 m. The muds of the lagoon are thought to be largely derived from the Guaíba River, chiefly because its large basin traps most of the river's sand (Toldo Jr., 1989; Toldo Jr. et al., 2003).

3. Location of cores and sampling

Two continuous cores, PT-04 (31°01′55″S, 51°18′04″W) and PT-06 (31°16′44.9469″S, 51°26′36.12122″W), were retrieved with gravity core system (Fig. 2a). Both cores (PT-04 and PT-06) are located in the central area of the Lagoa dos Patos and far from the mouths of the Guaíba and Camaquã rivers. The PT-04 core is ~30 km from the mouth of the Camaquã river, and the PT-06 core is 60 km from the mouth of the Guaíba river. Both rivers export suspended sediments to Lagoa dos Patos, mainly the discharge from the Guaíba river. Cores were collected during fieldwork in February of 2014 using a 5-m-long coring chamber to extract it and they contain well-preserved sediments. Sediments are characterized by dark gray to brown muds (Fig. 2b).

The seismically muddy layer between the sediment-water interface and the sub-bottom reflector contains the Holocene lagoonal sequence (Toldo Jr. et al., 2000; Bortolin et al., 2018). From the transition between the margins and the floor of the lagoon, this layer increases in thickness to about 6 m. Texturally, this transparent layer, as yet not totally penetrated by the gravity core, likely consist of almost pure mud, whose depositional environment was the low-energy bottom of the lagoon (Toldo Jr. et al., 2000). Muddy deposits have a flat bottom, with sediments ranging from silt to silty clay. They are homogeneous, organic rich and seismically transparent (Toldo Jr. et al., 2000).

Six ^{14}C age determinations presented by Toldo Jr. et al. (2000) for the top 2 m of mud yielded an uncompacted average sedimentation rate of 0.52 ± mm/yr, which compares broadly with the rate of 0.75 ± mm/yr based on stratigraphic projection. The short-term rates of sedimentation calculated in two cores by ^{210}Pb measurements (Martins et al., 1989) are quite different. Martins et al. (1989) used samples from the uppermost 10 cm of the cores and obtained rates of 3.5 and 8.3 mm/yr,
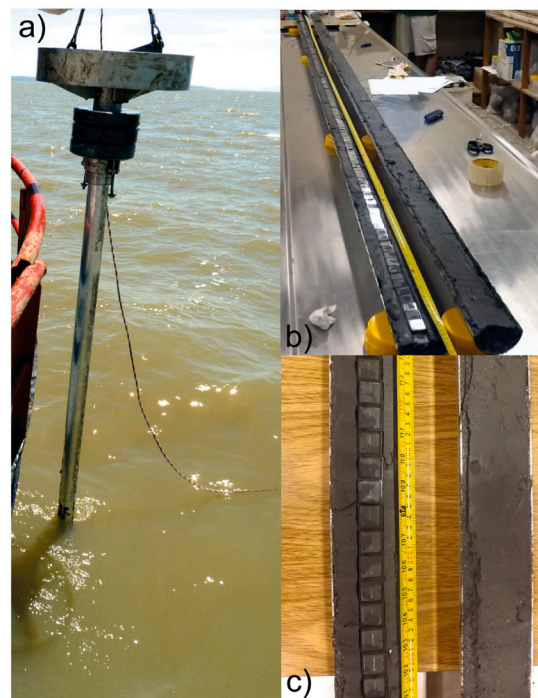

Fig. 2. (a) Field photograph of the operation on the boat. (b) Split core on the working table for measurement and collecting paleomagnetic samples. (c) Archive and working halves of the core PT-06 with 8 cm^3 paleomagnetic boxes pushed into the sediment in the middle of the core (sampling in b) and c) was performed in the laboratory out in the laboratory Universidade Federal do Rio Grande do Sul - UFRGS. The oceanographic research expedition in was conducted by Laboratório de Oceanografia e Geofísica Marinha (LOGMAR/CECO/UFRGS) in February of 2014, for collection of samples on the lagoon floor, for studies on the sedimentation rate and isotopic signature.

which are nearly ten times higher than those obtained for the older sediments. These high sedimentation rates could result from deforestation in the drainage basin since European colonization, which started about 150 years ago.

4. Methods

4.1. Sub-sampling

In November of 2014, sediment cores were opened for description and subsampling. Paleomagnetic specimens from the sediment cores were collected using cubic plastic boxes (8 cm^3) placed side-by-side continuously orientation towards the top of each core (Fig. 2c). A total of 218 cubic samples (132 for PT-04 and 86 for PT-06) were pushed into the split core faces so that samples were taken one next to the other (~2.5 cm resolution).

4.2. Dating

Chronological framework is based on accelerator mass spectroscopy (AMS) radiocarbon ^{14}C dating of 11 samples distributed between cores PT-04 (7 samples) and PT-06 (4 samples) (Table 1 and Table 2). Dating was performed at the Radiocarbon Laboratory of the Physics Institute at the Universidade Federal Fluminense (LAC-UFF) and at the Beta Analytic Inc. Carbon ages were calibrated to calendar years using the SHCal20 calibration curve (Hogg et al., 2020). Age-depth models were settled through the Bacon methodology (Blaauw and Christen, 2011) using the Rbacon 2.5.3 package (*The Comprehensive R Archive Network*, https://cran.r-project.org/).

4.3. Paleodirection and paleointensity determinations

All paleomagnetic and rock magnetic measurements were carried out at Laboratório de Paleomagnetismo (USPMag) at the University of São Paulo (USP), Brazil. Remanence measurements were conducted out using a three-axis 2-G Enterprises cryogenic magnetometer (model 755R), housed in a magnetically shielded room. All 218 samples were submitted to stepwise alternating field demagnetization (AFD) over 17 steps: 0, 2, 4, 7, 10, 15, 20, 25, 30, 35, 40, 50, 60, 70, 80, 90, 100 mT. Stable characteristic remanent magnetization (ChRM) directions (declination and inclination) were identified through visual inspection of orthogonal demagnetization plots (Zijderveld, 1967), and were calculated by fitting linear trends in demagnetization plots using principal component analysis (PCA, Kirschvink, 1980). A minimum of 6 demagnetisation steps were used to define the ChRM.

After AFD treatments of each sample, anhysteretic remanent magnetization (ARM) was imparted in a 100 mT AF with a direct current bias field of 0.05 mT. ARM was then demagnetized with the same AFD steps used to demagnetize the natural remanent magnetization (NRM).

These measurements enabled us to estimate the relative paleointensity through the pseudo-Thellier method of Tauxe et al. (1995). The pseudo-Thellier method works as a normalization and has been widely used in sediment cores (Tauxe et al., 1995; Brachfeld and Banerjee, 2000; Irurzun et al., 2009). In this method, the NRM remaining at each demagnetization step is compared with the ARM acquired in the corresponding demagnetizing field. It shows some advantages compared to the classical normalization method, as it allows one to compare the NRM and ARM contained in the same coercivity range, and provides a more effective way of eliminating the viscous remanent magnetization (VRM) component. The magnetic parameter ARM at 100 mT is also related to the concentration of single domain (SD) and pseudo-single domain (PSD) or vortex grains. In this work, the relative paleointensity curve determined by the pseudo-Thellier method was compared to those resulting from the classical normalizations by magnetic susceptibility (χ), ARM and saturation of isothermal remanent magnetization (SIRM).

4.4. Rock magnetism experiments and X-ray diffraction

Magnetic susceptibility was measured using an MFK1-FA Multi-Function Kappabridge at two operating frequencies (976 and 15,616 Hz), in a field of 200 A/m. Samples were also submitted to a pulse field of 900 mT (SIRM or IRM$_{900mT}$) and stepwise demagnetized, following the same steps used for NRM and ARM demagnetization. Then, a reverse field of 300 mT (IRM$_{-300mT}$) was applied to these samples. This routine was performed with a 2G Enterprises Pulse Magnetizer, and remanence was measured with the three-axis 2G Enterprises cryogenic magnetometer (model 755R). From these measurements, we calculated the S-ratio (S$_{300mT}$ = [IRM$_{-300mT}$/IRM$_{900mT}$]) and "hard" isothermal remanent magnetization (HIRM = [IRM$_{900mT}$ + IRM$_{-300mT}$]/2) parameters (Thompson and Oldfield, 1986; Bloemendal et al., 1988). S-ratio is used to indicate the relative concentration of low versus high coercivity minerals (Thompson and Oldfield, 1986; Bloemendal et al., 1988). HIRM has been used as a proxy for the concentration of high coercivity minerals. HIRM is a concentration parameter rendering an intensity of magnetization carried by minerals, in the present case, with coercivities between 300 mT and 900 mT. The concentration of high-coercivity magnetic minerals, i.e., hematite/goethite can also be inferred from the HIRM (Bloemendal et al., 1992; Liu et al., 2007). Another calculated parameter was the IRM$_{900mT}$/χ ratio, often used to make inferences about the grain-size variation of magnetic minerals (e.g., Peters and Dekkers, 2003). We also calculated the median destructive field of the NRM (MDF), which provides a rough estimate of relative grain-size of magnetic particles for a uniform magnetic mineral assemblage. All magnetic measurements can be found in appendix A.

A fraction of ~1 g of sediment was collected from 28 representative samples PT-04 and 16 representative samples from PT-06 for hysteresis loops measurements. The number of samples represented is proportional to the total number of samples from each core, that is, hysteresis

Table 1
Radiocarbon age determinations and calibrated age ranges for PT-04 core. The table shows the types of materials used for dating, the laboratory where this procedure was performed, the depth of each sample and the ages found.

Material	Lab code	Depth (cm)	^{14}C age (years BP)	Median cal age (years BP)	Maximum (2σ BP)	Minimum (2σ BP)
Erodona mactroides; Heleobia sp.; Cirrípede; Acteocina bidentata; Mactra isabelleana;	LACUFF-180011	50	3319 ± 29	3491	3573	3400
Erodona mactroides; Clausinella gayi;	LACUFF-180012	110	3572 ± 29	3820	3958	3697
Corbula sp.; Heleobia sp.; Acteocina bidentata;	Beta-424,874	150	3820 ± 30	4162	4344	3990
Mactra isabelleana; Heleobia australis; Acteocina bidentata;	LACUFF-180013	200	3772 ± 30	4087	4233	3935
Erodona mactroides; Heleobia sp.; Corbula sp.; Acteocina bidentata	Beta-424,875	250	4080 ± 30	4515	4791	4417
Acteocina bidentata; Nucula semiornata; Clausinella gayi; Heleobia sp.;	LACUFF-180014	300	3947 ± 28	4340	4507	4162
Nucula semiornata;	Beta-424,876	370	4260 ± 30	4744	4858	4620

Table 2
Radiocarbon age determinations and calibrated age ranges for PT-06 core. The table shows the types of materials used for dating, the laboratory where this procedure was performed, the depth of each sample and the ages found.

Material	Lab code	Depth (cm)	^{14}C age (years BP)	Median cal age (years BP)	Maximum (2σ BP)	Minimum (2σ BP)
Corbula;	LACUF-180005	120	3146 ± 27	3308	3388	3221
Clausinella gayi; Heleobia sp.; Mactra isabelleana;	LACUF-180006	150	3311 ± 27	3479	3569	3398
Mactra isabelleana; Erodona mactroides; Heleobia sp.	LACUF-180007	200	3477 ± 29	3706	3830	3593
Mactra isabelleana;	LACUF-180008	320	3967 ± 27	4362	4513	4245

measurements were performed in about 20% of the samples from each core. These results allow one to identify the domain state(s) and magnetic interactions among magnetic particles (Day et al., 1977; Dunlop, 2002). We measured hysteresis loops and IRM acquisition curves up to 1 T at room temperature using a vibrating sample magnetometer (VSM MicroMag™ 3900).

Mineralogy was also investigated through X-Ray powder Diffraction (XRD) in some representative samples (Fig. S1). Approximately 1 g of powder from each sample was dried in a 40 °C laboratory oven for 8 h. XRD was performed using an Empyrean Panalytical diffractometer with spinner, Cu Kα radiation, operated at 40 mA and 40 kV, range of 2q from 5° to 80°, and a 0,01° 2q step size. The software HighScore Plus (4.8 version) was used for mineral identification, alongside the International Center for Diffraction Data (ICDD) and the Crystallography Open Database (COD). The combined XRD analysis from the Epsilon 1 Panalytical Omnian module also contributed for mineral identification.

5. Results

5.1. Rock magnetism and XRD data

Magnetic susceptibility (χ) for the PT-04 increases almost continuously down core from ~3 × 10^{-8} m^3/kg to ~4.5 × 10^{-8} m^3/kg (Fig. 3a). Some susceptibility peaks occur in the upper half of core PT-04 at approximately 62 cm, 83 cm, 85.5 cm and 144.5 cm depth. For PT-06 core, the values are roughly constant throughout the core, with a mean value of 3.13 × 10^{-8} m^3/kg (Fig. 3f) that is similar to the mean susceptibility value for the uppermost 300 cm of core PT-04 (Fig. 3a). In this core, a peak value reaching 3.94 × 10^{-8} m^3/kg is observed in the lower half of the core at ~249 cm dept.

S-ratio remains remarkably constant throughout both cores with values around 0.83 in PT-04 (Fig. 3b) and 0.81 in PT-06 (Fig. 3g), which indicate a mixture of low- and high-coercivity magnetic minerals (Liu et al., 2007). A small decrease in S-ratio is observed at ~110 cm (PT-04, Fig. 3b) and 245 cm (PT-06, Fig. 3g). We also observe an increase at 286 cm in PT-06 core (Fig. 3b), which is indicative of an increment of a relatively higher proportion of soft magnetic grains.

Oscillations of the ARM at 100 mT intensities throughout the cores are limited, with values comprised within the same order of magnitude (around 4.06 × 10^{-7} Am^2/kg for PT-04 and around 3.66 × 10^{-7} Am^2/kg for PT-06; Fig. 3c,h). The maximum and minimum ARM values for the PT-04 core are 5.96 × 10^{-7} Am^2/kg to 2.97 × 10^{-7} Am^2/kg, respectively. ARM varies between 6.36 × 10^{-7} Am^2/kg and 1.98 × 10^{-7} Am^2/kg through the PT-06 core (Fig. 3h).

HIRM varies around 1.36 × 10^{-4} Am^2/kg in the PT-04 core and 1.50 × 10^{-5} Am^2/kg in the PT-06 core (Fig. 3d,i). The IRM$_{900mT}$/χ ratio has relatively constant values around 0.5 and 0.6 A/m A/m throughout cores PT-04 and PT-06, respectively (Fig. 3e,j).

Hysteresis data (Fig. 4; Table S1), including the ratio of saturation remanence to saturation magnetization (M_{rs}/M_s) and the coercivity of remanence to coercive force (H_{cr}/H_c) from PT-04 (Fig. 4a) and PT-06 (Fig. 4b) samples lie within the pseudo-single domain (PSD) field of

Day et al. (1977) or vortex state of Roberts et al. (2018). The presence of magnetite mixed with hematite suggested by the S-ratio is further confirmed by the wasp-waisted shape of the loops (Roberts et al., 1995; Tauxe et al., 1996). The linearity of the χ versus SIRM (Fig. 4f) for both cores implies that grain-size does not change significantly across the sedimentary column (Gogorza et al., 2018) excepted for few samples.

The similarity in mineralogical composition across the stratigraphy is also indicated by the XRD patterns obtained for samples from depths from 149 and 359 of PT-04 and 251 and 320 of PT-06 (Fig. S1), with very small differences between samples. The samples PT-06-107-251 (Fig. S1a), PT-06-136-320 (Fig.S1b), PT-04-063-149 (Fig. S1c) and PT-04-152-359 (Fig. S1d) are constituted mainly by Gypsun, Kaolinite, Quartz and Titanomagnetite.

5.2. Age model

Age-depth models for PT-04 and PT-06 are shown in Fig. 5. It is observed that the three ages carried out at the Beta laboratory, for the samples from PT-04, indicate a trend of older ages compared to the trend indicated by the ages carried out at the LAC-UFF laboratory. However, we do not have enough evidence to decide if the dates obtained by one of the laboratories would be more reliable than the dates carried out in the other laboratory. In this context, we choose to use all the dates in the construction of the age models.

Thus, the age-depth models for PT-04 and PT-06 (Table 1 and Table 2) cover time intervals from 4541 cal years BP to 3794 cal years BP and from 4345 cal years BP to 3320 cal years BP, respectively (Fig. 5). Therefore, there is an overlap of data between 4345 and 3794 cal years BP, corresponding to ~550 years. The mean values of the 95% confidence levels for the age models were 201 years for PT-04 and 233 years for PT-06. Depth scales were then converted into age using the independent radiocarbon-based age models for each core. For the core PT-04, a cubic sample represents approximately ~5,64 years of deposited sediment. In the PT-06, we have ~11.9 years in each cubic sample of deposited sediment. These results demonstrate that short-lived features in geomagnetic field behaviour can be recorded in our data.

5.3. Paleodirection records

Stepwise AFD of the NRM indicates a stable primary remanent magnetization that is directed towards the origin after elimination of a VRM in most samples. Paleomagnetic directions were calculated by fitting a linear regression line to minimize the maximum angular deviation (MAD) that remained below 14° in PT-04 core and 6.5° in PT-06 core (Fig. 6). These low MADs attest to the quality of the calculated ChRM directions (e.g., Stoner and St-Onge, 2007).

Fig. 7 shows the rock magnetism and paleomagnetic results for both cores. Cores PT-04 and PT-06 are azimuthally unoriented and thus no absolute declination values could be obtained. Because of that we represented the relative declinations centered around the mean declination for each core (Fig. 7e,k). Relative declinations for core PT-04 range between −26.1° and 32.8° with a mean value of about −1.9°. For core
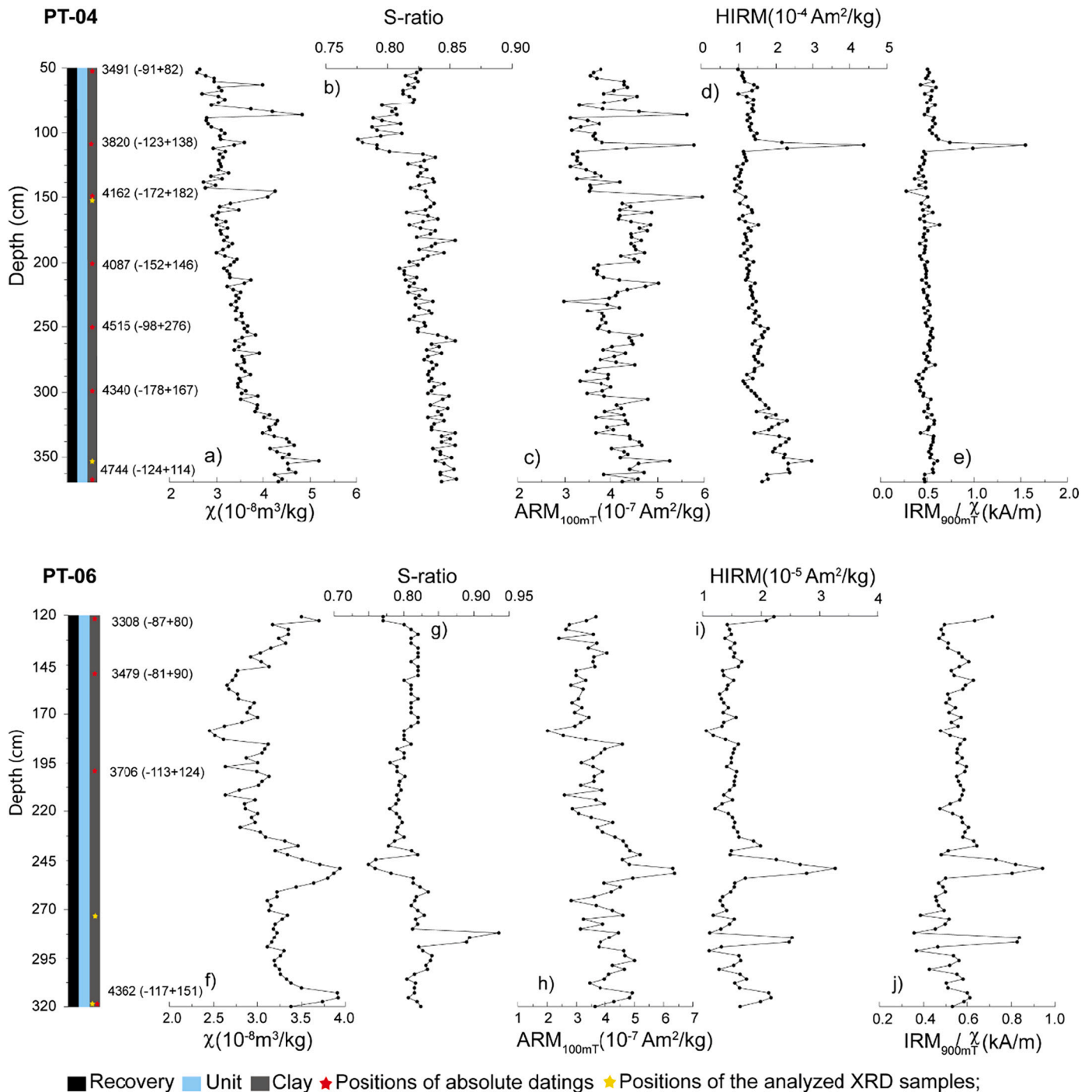
Fig. 3. Depth variations of magnetic susceptibility, S-ratio, ARM, HIRM, and IRM900$_{mT}$/χ for cores PT-04 and PT-06. Positions of AMS radiocarbon dates used to construct the age models are indicated star shaped.

PT-06, relative declinations range between −15° and 25.3° with a mean value of about 0.16°. The mean inclination for core PT-04 is −39,6° (Fig. 7f); inclinations range between −8,8° and − 58.5°. For core PT-06, inclination varies from −25.6° to 51.5° around a mean of −38.4° (Fig. 7l). The difference may be due to the cores not being oriented. So these declination values are relative.

Median destructive fields (MDFs) for cores PT-04 and PT-06 are 19.6 mT and 15.7 mT, respectively. Values of IRM$_{900mT}$/χ from the PT-06 core resemble lower MDFs correspondent to lower IRM$_{900mT}$/χ values and, hence, to coarser magnetic grains. However, for the PT-04 core, this correlation is not so evident (Fig. 7b,d).

We then performed a stacking of individual curves with the aim to obtain more reliable estimates of the temporal variation in the directions of the geomagnetic field (Gogorza et al., 1999, 2000a, 2000b, 2002, 2012; Irurzun et al., 2006, 2008). To calculate the stacked curves, each data series was initially interpolated every 10 years. This sampling interval was chosen because it is compatible with the average temporal resolutions of each of the cores (~ 6 years for PT-04 and ~ 12 years for PT-06). After, the stacked curves were calculated from the averaged values of the data recorded in the two cores for each age of the overlapping period (4340 to 3800 cal years BP). The final inclination and declination records for both cores and the stacked profile of arithmetic
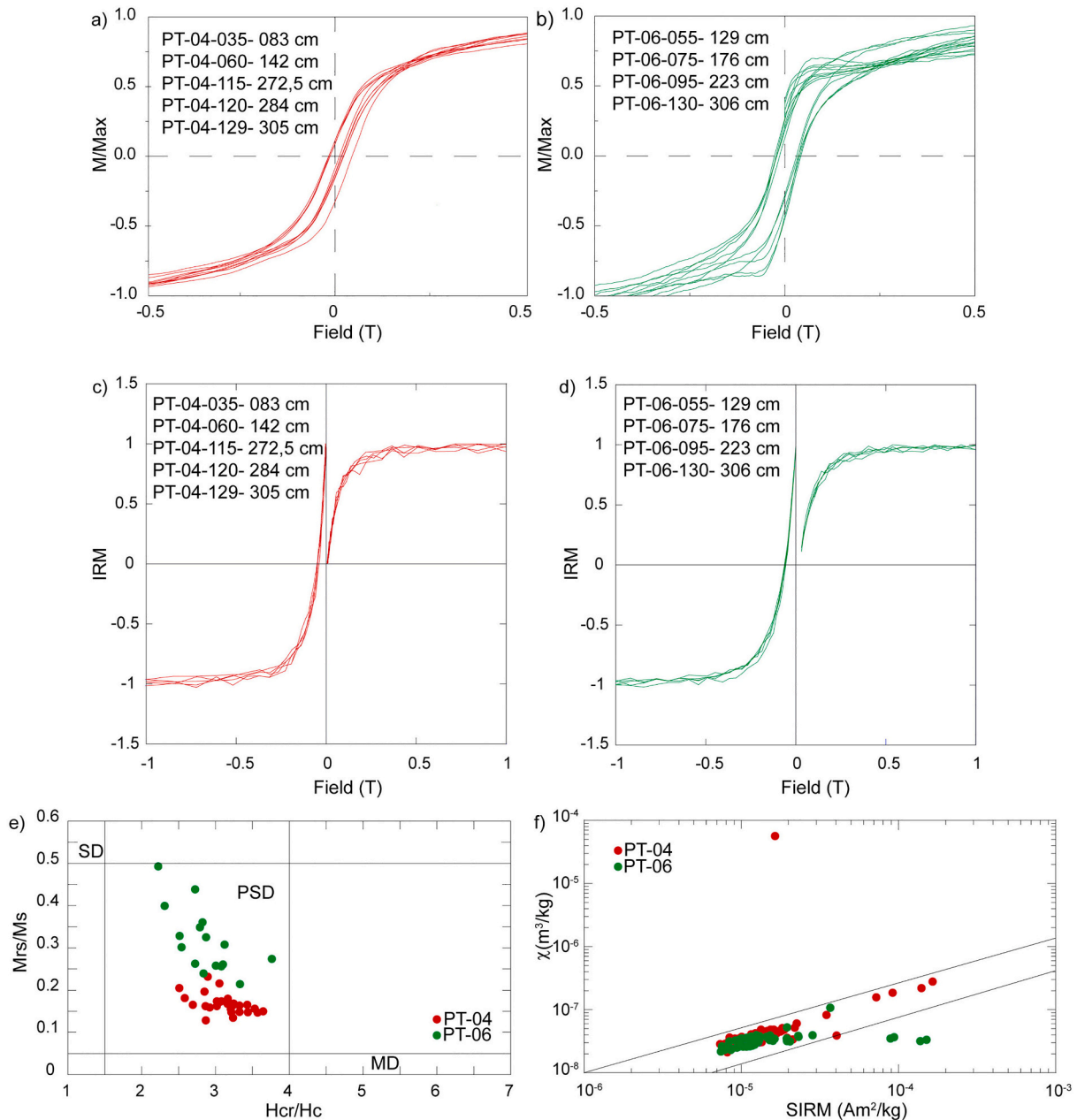
Fig. 4. Representative hysteresis loop for the studied Lagoa dos Patos sediments; (a) samples of core PT-04 and (b) samples of core PT-06. Isothermal Remanent Magnetization (IRM) acquisition curves, for representative samples from cores PT-04 (c) and PT-06 (d). Day diagram (Day et al., 1977) for samples from cores (e) (SD - Single Domain; PSD - Pseudo-Single Domain; MD - MultiDomain data fields). Susceptibility (χ) versus Saturation of the Isothermal Remanent Magnetization (SIRM) for all samples in order to estimate concentration and grain size, according to (Thompson and Olfield, 1986).

averages for the overlapping period are plotted versus age in Fig. 8. The values of the Pearson's correlation coefficient for inclination and declination data of both cores are −0.15 and 0.22, respectively. These low correlation values obtained can be attributed to differences between the age models of each core, local depositional characteristics, and to different magnetization lock-in.

5.4. Relative paleointensity records

Sediments from PT-04 and PT-06 cores are ideal for recovering relative paleointensity data because they have small variations in the rock magnetic parameters throughout the record (less than a factor of 10, Fig. 3). Rock magnetic results demonstrate the well-defined magnetization is carried by PSD magnetite and titanomagnetite

(Fig. 4). We have used the normalization techniques of Tauxe (1993) to calculate the relative paleointensity (RPI) records from the two study cores. These techniques consist of normalizing the measured NRM by an appropriate parameter in order to compensate for the variable concentration of ferrimagnetic materials (e.g., Tauxe, 1993). We chose the 15mT-level to quantify RPI estimates from NRM, ARM, and SIRM, in order to eliminate the viscous component of relatively low magnetic stability as proposed by Levi and Banerjee (1976). Relative paleointensity records for our two studied cores are shown in Fig. 9. We have normalized the NRM_{15mT} by the magnetic susceptibility (χ), ARM_{15mT}, and $SIRM_{15mT}$ (Fig. 9a-c). We have also obtained paleointensity with the pseudo-Thellier method (Tauxe et al., 1995) (Fig. 9d). All magnetic methods attempted here produced similar results, but differ in amplitude of peaks (Fig. 9). The resemblance between the results of
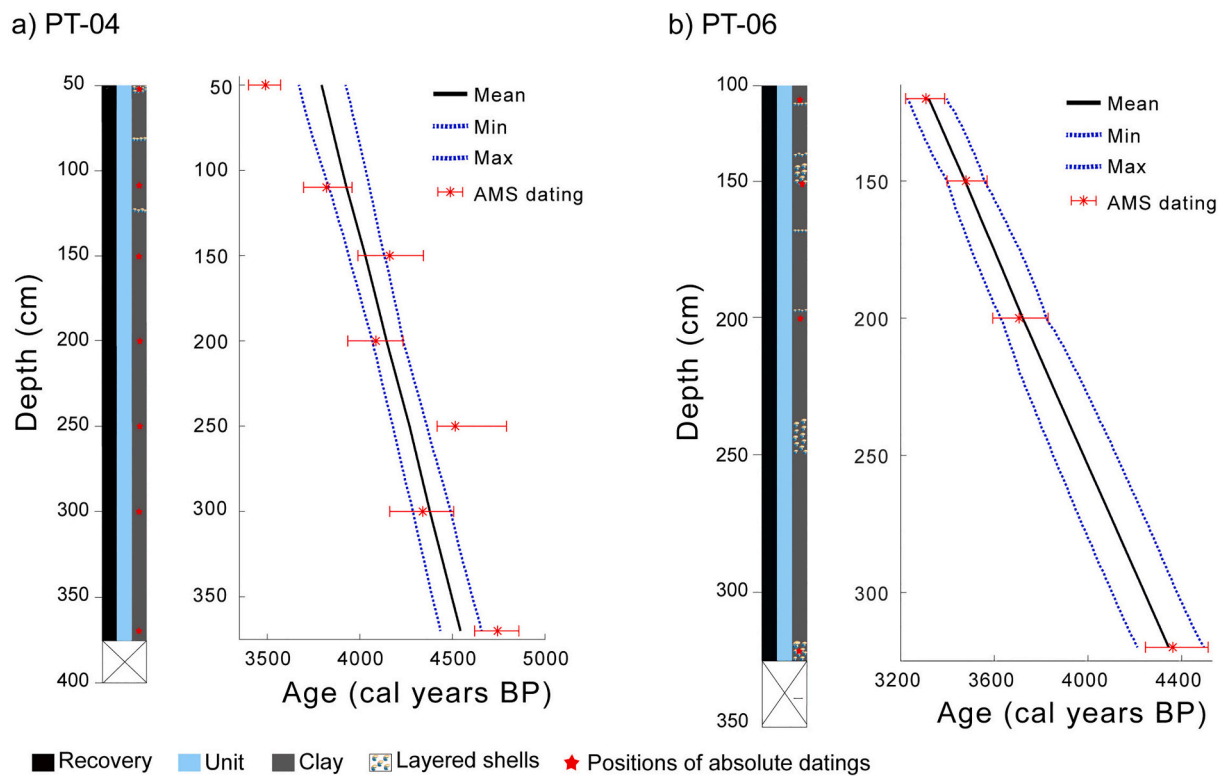
Fig. 5. Age models for cores (a) PT-04 and (b) PT-06. The age models are based on AMS radiocarbon dating ([Table 1](#) and [Table 2](#)). Lithostratigraphic columns of the studied Holocene sediments from Lagoa dos Patos, cores (a) PT-04 and (b) PT-06. Positions of AMS radiocarbon dating used to construct the age models are indicated star shaped in the lithostratigraphic columns.

normalized parameters and the pseudo-Thellier, for the same core, suggests that these determinations are robust and were not significantly affected by the viscous component (e.g., [Tauxe, 1993](#); [Tauxe et al., 1995](#); [Gogorza et al., 2006, 2008](#)). For the overlapping period the Pearson's correlation coefficient for stacked curves of both cores are 0.21 (for $NRM_{15mT}/SIRM_{15mT}$), 0.05 (for NRM_{15mT}/χ), 0.02 (for $NRM_{15mT}/SIRM_{15mT}$) and 0.05 (for pseudo-Thellier). Low correlation values can be associated to the same factors previously mentioned in the presentation of inclination and declination results.

Stack parameters show RPI variations from 4540 and 3320 cal years BP. Slightly higher values of RPI parameters are observed in these levels (4430–4330, 4230–4130, 3630–3530, and 3430–3330 cal years BP, respectively). All data can be found in appendix A.

6. Discussion

6.1. Paleosecular variation

Continuous directional paleomagnetic data for the Late Holocene are scarce in South America. There are only a few records obtained from the lake sediments of Argentina ([Gogorza et al., 2002](#); [Irurzun et al., 2006](#); [Gogorza et al., 2012, 2018](#)) and stalagmite from Brazil ([Jaqueto et al., 2022](#)). Although these lakes are located >2000 km from Lagoa dos Patos, at a distance where regional differences in the sub-millennial geomagnetic field ([Korte et al., 2019](#)) changes are expected, they provide the closest PSV curves that can be used in the correlation. The cores PT-04 and PT-06 showed sedimentation rates of lower variability over time in comparison with cores that are close to the river and estuarine outlets, indicating comparatively constant sedimentation conditions. [Fig. 10](#) shows the comparison between Lagoa dos Patos stacked data and lacustrine records from Lake Escondido (41°S, 71°30′W; [Gogorza et al., 2002](#)), Lake El Trébol (41°04′S, 71°29′W; [Irurzun et al., 2006](#)), Laguna Potrok Aike (51°58′S, 70°23′W; [Gogorza et al., 2012](#)), Lake Carmen

(53°40′S 68°18′W; [Gogorza et al., 2018](#)) and the SHADIF.14 k and CALS10k models available for each latitude. We also present in [Fig. 10](#) the error data for the SHADIF.14 k model, where the shading (in light green) means the minimum and maximum values and also for the curve of our records where we have a period in common between PT-04 and the PT-06 (3800–4530 cal years BP); maximum and minimum values are represented by the orange shading. The other records do not provide this error data. The difference between the sampling rates used in the different studies is striking. Sedimentation rate is comparable only with records from Laguna Potrok Aike but data exhibits different tendencies. However, the variability is higher in the Lagoa dos Patos records ([Fig. 10](#)).

Inclination and relative declination values for cores PT-04 and PT-06 are consistent between consecutive samples and reveal gradually varying directional changes ([Fig. 8](#)). These changes appear to be unrelated to variations in lithology or rock magnetic properties ([Fig. 3](#) and [Fig. 4](#)). The mean paleomagnetic inclination for the stacked curve (−38.3°) is 11.9° shallower than the expected inclination for a geocentric axial dipole (GAD) field (−50.2°) at studied locality ([Fig. 8](#)a). The observed inclination flattening is expected where the ChRM is a detrital remanent magnetization (e.g., [Tauxe, 2005](#); [Tauxe et al., 2008](#)). The highest variation in the inclination record occurs when the magnetic inclination increases from approximately 4530 cal years BP until approximately 4300 cal years BP, followed by a progressive decrease from about −20° to near −50° in 4230 cal years BP. Mean inclination values observed in our data are lower than the values observed in Argentinian data. This is expected due to the latitudinal difference between locations. Furthermore, inclination data from Lagoa dos Patos present a long-term trend of increasing values. On the other hand, data of Escondido, El Trébol and Potrok Aike show a long-term trend of decreasing inclination values.

Inclination and relative declination records from Lagoa dos Patos are plotted together with the predictions from the global geomagnetic models CALS10k.2 ([Constable et al., 2016](#)) and SHA.DIF.14 k ([Pavón
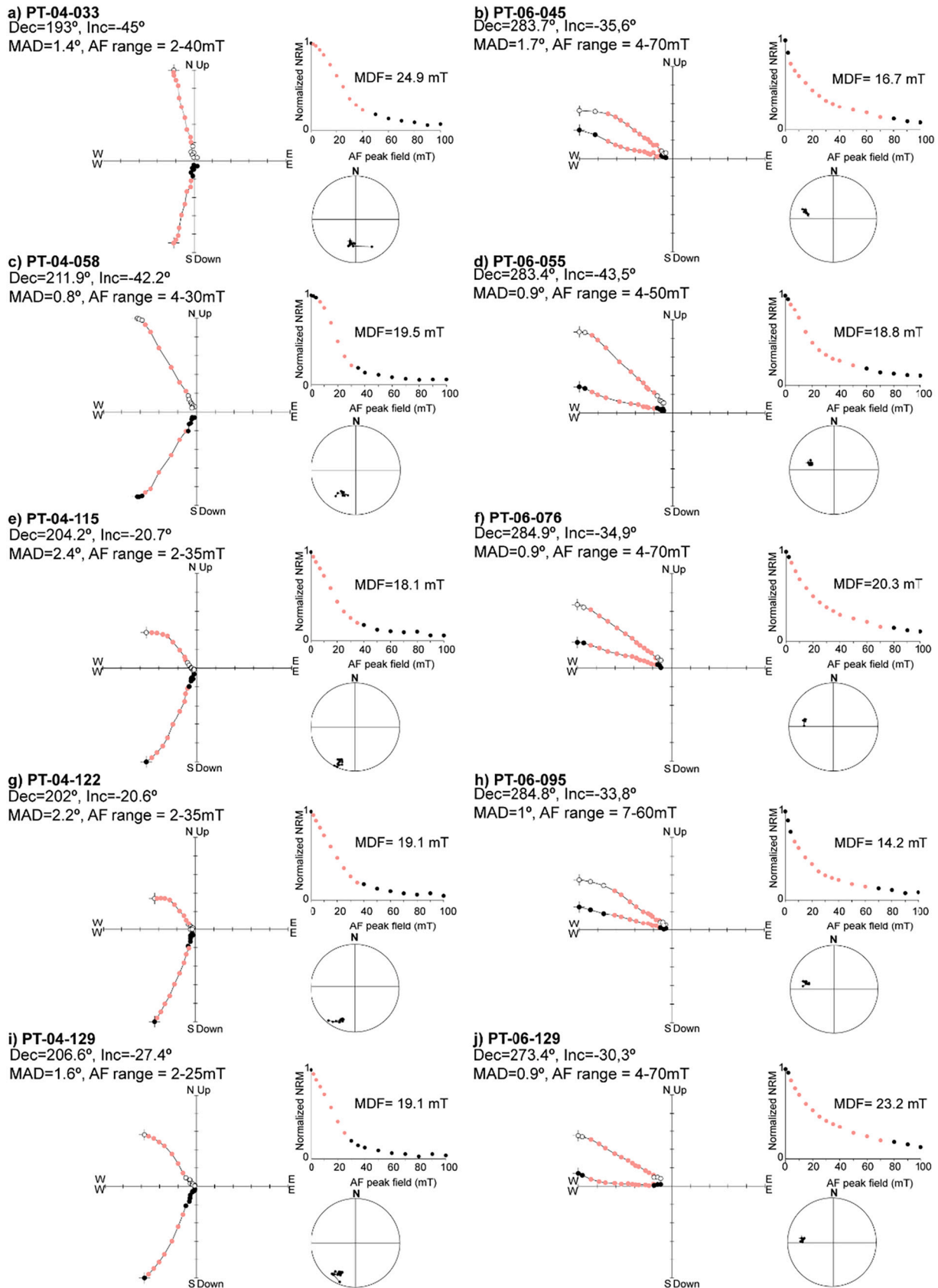
Fig. 6. AF demagnetization results for representative samples from cores PT-04 and PT-06. In the Zijderveld (1967) diagrams, open (closed) circles represent projections onto the vertical (horizontal) planes. Corresponding stereographic projections and normalized NRM-intensity decay curves are also shown. Numbers indicate the range of AF applied corresponding to the characteristic remanent magnetization (ChRM) used to calculate the paleomagnetic directions (pink circles indicate the demagnetization steps) and MDF determined for each sample. (For interpretation of the references to colour in this figure legend, the reader is referred to the web version of this article.)
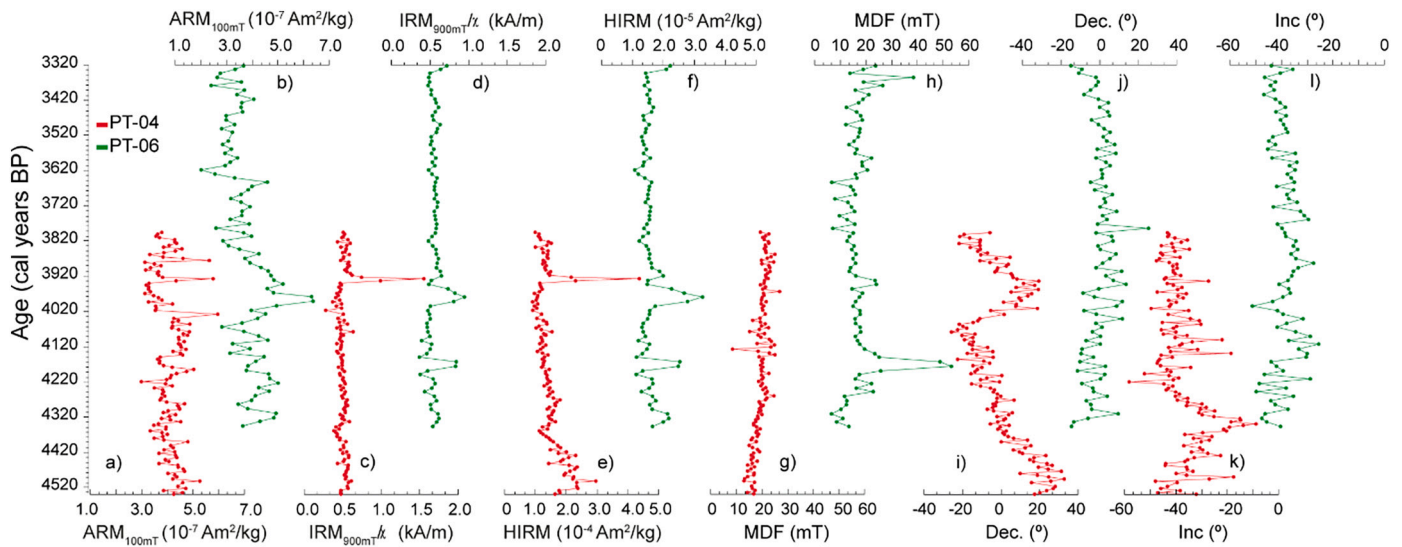
Fig. 7. Age-depth variations of ARM, IRM$_{900mT}$/χ, HIRM, median destructive field (MDF) and relative declination and absolute inclination of the characteristic remanent magnetization (ChRM) directions obtained for cores PT-04 (red) and PT-06 (green). (For interpretation of the references to colour in this figure legend, the reader is referred to the web version of this article.)
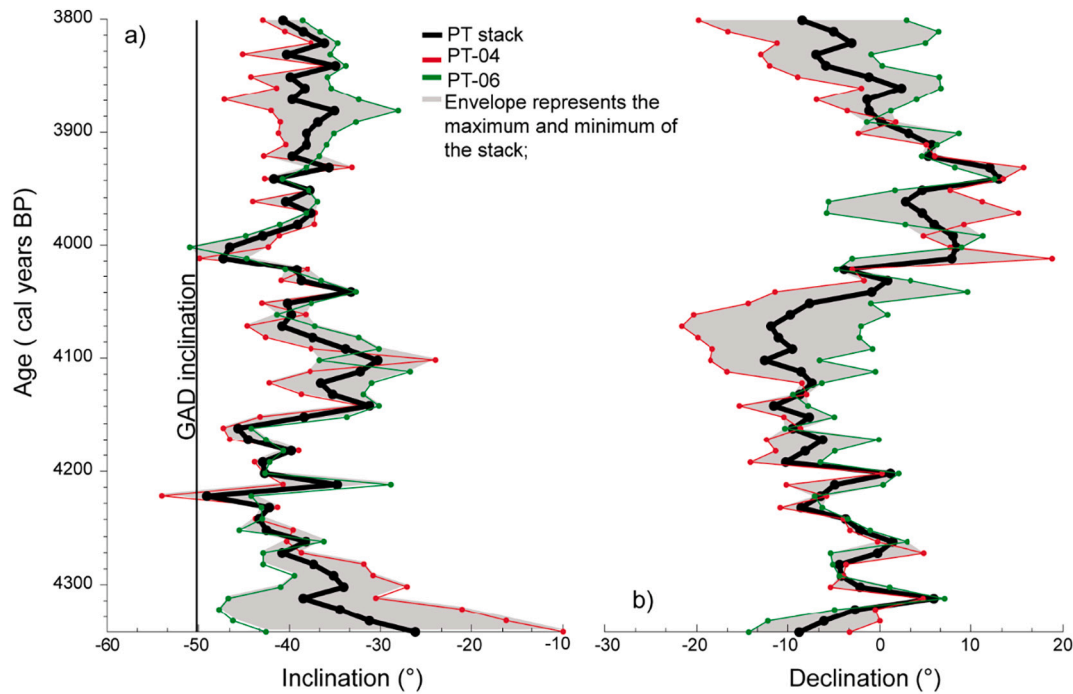

Fig. 8. Inclination and relative declination for cores PT-04 (red) and PT-06 (green) and stacked profile (black). Gray shading represents the minimum and maximum values of the stacket profile. The inclination expected for a geocentric axial dipole (GAD) field at site latitude is indicated by a black line. (For interpretation of the references to colour in this figure legend, the reader is referred to the web version of this article.)

Carrasco et al., 2014) (Figs. 10, 11). The CALS10k.2 model is based on lake sediment data and provides a representation of the large-scale field at the core-mantle boundary. The SHA.DIF.14 k model is based on archeomagnetic data (including lava flow and archaeological artefacts data) and presents a greater variation in spatial and temporal terms compared to the CALS10k.2 model. Inclination stack of the Lagoa dos Patos record presents similar trends when compared with SHA.DIF.14 k model from approximately 4540 and 4130 cal years BP. This correlation also occurs for ~100 years in the top of the section, between 3430 and 3330 cal years BP. In the rest of the record (~700 years), the inclination of the Lagoa dos Patos is lower than that predicted by models. Relative

declination of Lagoa dos Patos differs from models. However, between 3730 and 3320 cal years BP, the Lagoa dos Patos record is in agreement with the CALS10k.2 global model. Additionally, inclination values predicted by CALS10k.2 and SHA.DIF.14 k models are generally higher than the values obtained in South American cores. Superimposed to shorter variations, our data show a long-scale (secular or longer) pattern of variation. Although similarities are observed during some periods for some locations, in general the models are not able to adequately represent the observed inclination variations in South America for the studied time interval.

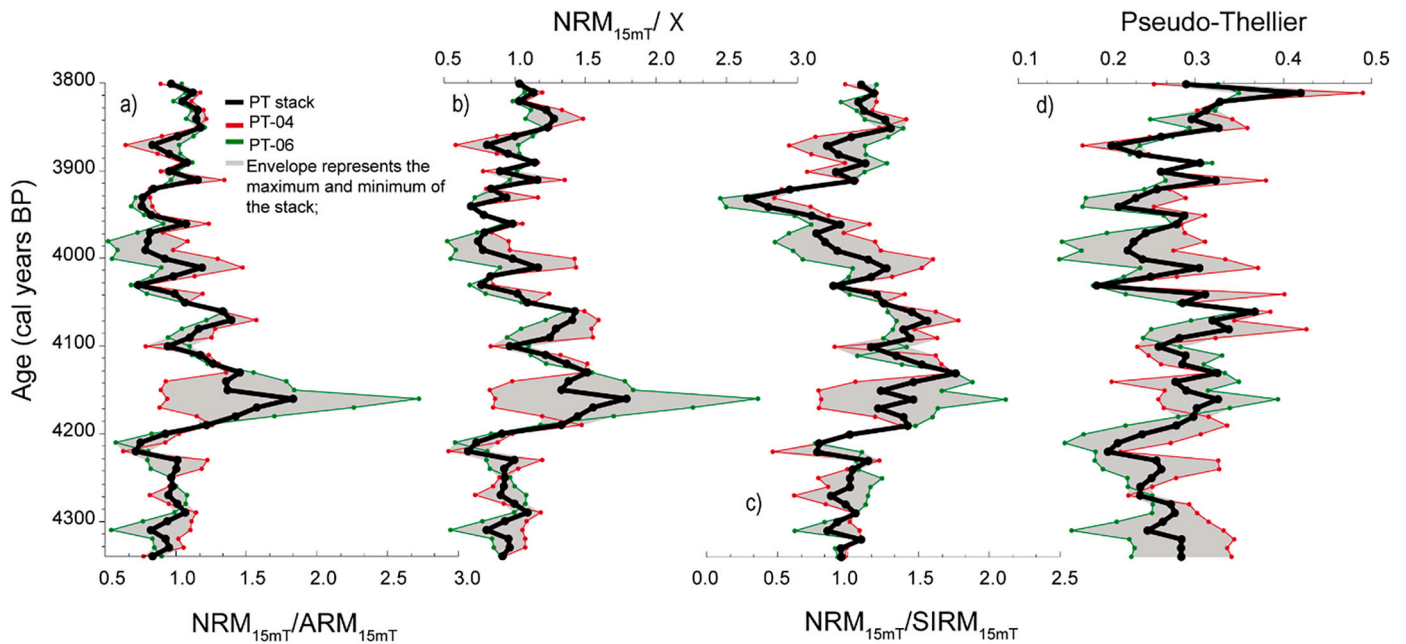To confirm the robustness of our inclination and relative

Fig. 9. Normalized estimates of relative paleointensity (RPI): a) $NRM_{15mT}/SIRM_{15mT}$, b) NRM_{15mT}/χ, c) NRM_{15mT}/ARM_{15mT} and d) curve of Pseudo-Thellier versus age. In red PT04, in green PT06, in black the stack profile and the gray shading represents the minimum and maximum values of the stack profile. (For interpretation of the references to colour in this figure legend, the reader is referred to the web version of this article.)

paleointensity data, we also compare with other high-resolution Holocene PSV records form Argentine lakes (Gogorza et al., 2002; Irurzun et al., 2006; Gogorza et al., 2012, 2018), stalagmites (Trindade et al., 2018; Jaqueto et al., 2022), and models (Constable et al., 2016; Pavón Carrasco et al., 2014) (Fig. 11). With all data taken together, the Lagoa dos Patos results express a low inclination variation in the studied interval in comparison with South American data (Fig. 11a). These results suggest a period of low geomagnetic field variations, which is indicative of low intensity of non-dipole contributions, such as due to SAMA. Similar results are found in the stalagmite DBE50 from central Brazil (Jaqueto et al., 2022).

PSV differences between sedimentary records and global geomagnetic models are largely reported in Holocene records. Two main factors may account (perhaps in combination) for the inferred differences. First, the Southern Hemisphere is with poorly represented, contributing with approximately 3% of the directional data used in the modeling and 5% of the intensity data (e.g., Donadini et al., 2009; Korte et al., 2009; Brown et al., 2015). Second, the model output is smooth and it does not take into account the variability observed in some localities. We plot the accuracy of the available SHADIF model for each lake in Argentina and Lagoa dos Patos in order to compare with the resolution of the lakes (Fig. 11).The significant differences of localized geomagnetic features originating from non-dipole fields (e.g. SAMA) reveals periods of relatively rapid directional changes ($>0.1°$ y^{-1}) (Tarduno et al., 2015; Hare et al., 2018; Trindade et al., 2018). Our data thus contributes to Holocene geomagnetic modeling efforts by adding new paleomagnetic direction data to the South American database.

6.2. Relative paleointensity variation

Our rock magnetic results from Lagoa dos Patos indicate that a well-defined magnetization component is carried by pseudo-single domain (PSD) or vortex magnetite and titanomagnetite. Magnetic concentration shows variations of less than a factor of 10, which is suitable for reconstructing the RPI curves (Tauxe, 1993). Furthermore, the remanence is carried by stable magnetite grains ranging in size from 1 to 15 μm (Fig. 4f). The normalization parameters must also take into account the variability in the contribution of the grain carrying the remanence,

which is controlled largely by changes in concentration and grain size (Figs. 3 and 4; Banerjee et al., 1981; King et al., 1982, 1983; Tauxe, 1993).

We compare our RPI data, calculated through NRM_{15mT}/ARM_{15mT} ratio, with the records from Argentina (Carmen Lake, Potrok Aike, El Trébol, Escondido; Gogorza et al., 2002, 2004, 2012; Irurzun et al., 2006) and with global geomagnetic models CALS10k (blue) (Brown et al., 2015; Constable et al., 2016) and SHA.DIF.14 k (green) (Pavón Carrasco et al., 2014) (Fig. 10). RPI results display a low variability compared to the geomagnetic field models (Figs. 10 and 11b). A tendency of increase in intensity at the beginning of the cores record from 4530 cal years BP to 4100 cal years BP is observed, followed by a decreasing intensity between 4100 cal years BP and 3680 cal years BP, and finally, an increase in intensities observed from 3680 cal years BP to 3330 cal years BP. However, the stacked RPI record shows a sharp high at about 4150 years (Fig. 10). This could be related to anomalously high values of the mean destructive field, HIRM and IRM_{900mT}/χ (Fig. 7) in the core PT-06. For this part of the core (~4100–4200 years) the pseudo-Thellier RPI (Fig. 9d) seems to be more reliable for normalizing the mineralogical and concentration changes as can be observed by the individual cores. However, our results show slow variations when compared with the stalagmites (Jaqueto et al., 2022). In Fig. 11b, we have superimposed the following records of relative paleointensity: Lagoa dos Patos stack (31°S), Potrok Aike (52°S) (Gogorza et al., 2012), Escondido (Gogorza et al., 2004), El Trébol (41°S) (Gogorza et al., 2006) and Carmen (54°S) (Gogorza et al., 2018) with the SHA.DIF14k and CALS10k models and also the absolute paleointensity records of stalagmites (Jaqueto et al., 2022). An intensity peak was observed in Lagoa dos Patos data around 3630 cal years BP. A similar peak was also recorded in the Lake Carmen data and is in agreement with the predictions of SHA.DIF14k model. Another intensity peak was also detected in South Brazil around 4180 cal years BP. This feature is also in agreement with SHA.DIF14k data. However, the model SHA.DIF14k did not predict the maxima intensity values observed in Lagoa dos Patos data around 3595 cal years BP and around 4380 cal years BP.

In general, our data shows high-amplitude variations in the RPI intensities, which differ from the smoothed variations predicted by global geomagnetic models (Fig. 10). However, the tendency of the RPI curve is
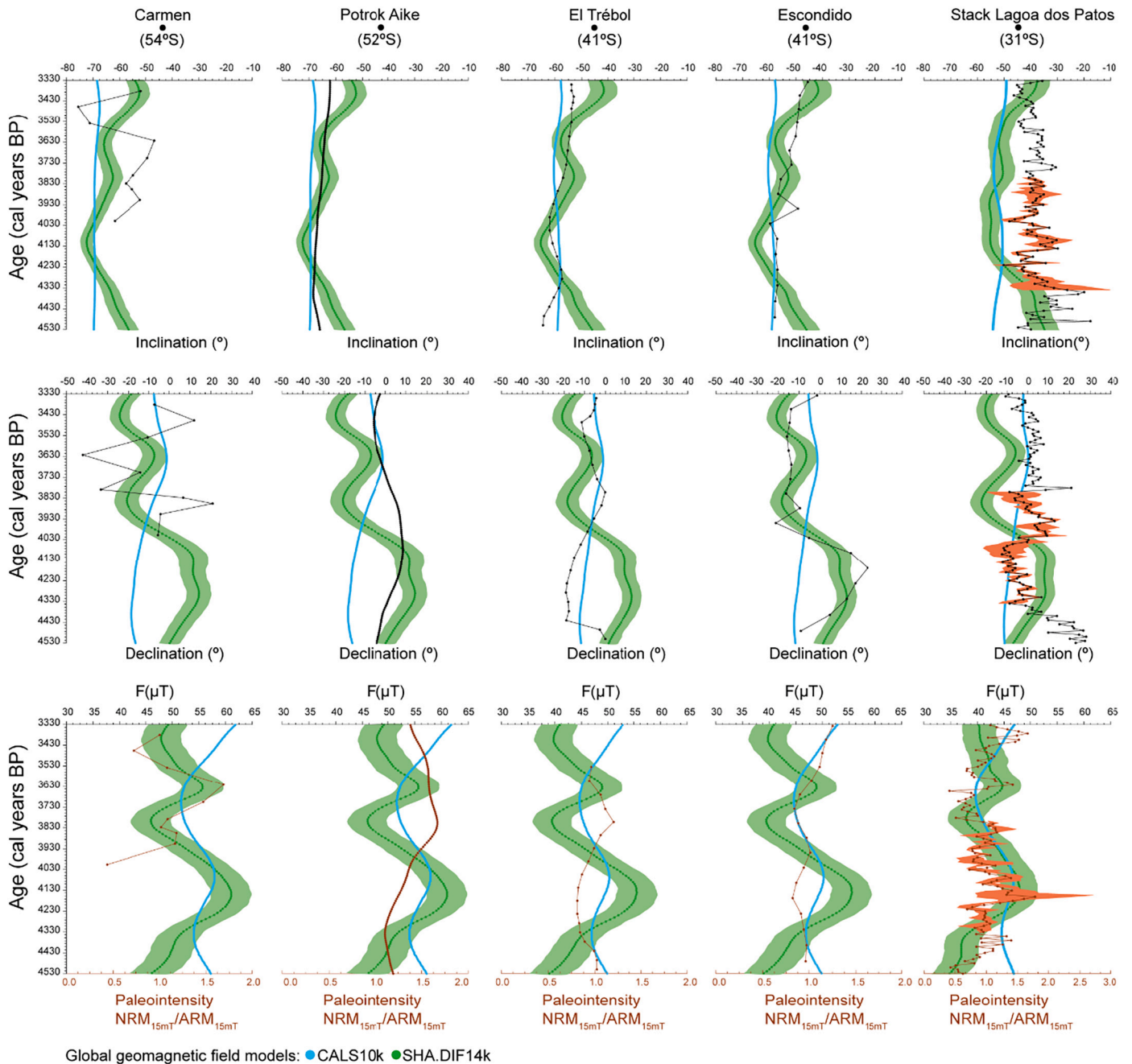
Fig. 10. Comparison of stacked inclination, declination and intensity logs from Carmen Lake, Potrok Aike, El Trébol, Escondido (Gogorza et al., 2002, 2004, 2012; Irurzun et al., 2006) and Lagoa dos Patos as a function of age with the theoretical models CALS10k (blue) (Brown et al., 2015; Constable et al., 2016) and SHA.DIF.14 k (green) (Pavón Carrasco et al., 2014) outputs. (For interpretation of the references to colour in this figure legend, the reader is referred to the web version of this article.)

very similar with the global geomagnetic models. Rapid field changes were observed in South America (Trindade et al., 2018) and South Africa (Tarduno et al., 2015; Hare et al., 2018). This is probably related to SAMA (e.g., Hartmann and Pacca, 2009), which is linked to reverse flux patches (RFPs) at the core–mantle boundary (CMB) (Terra-Nova et al., 2015; Terra-Nova et al., 2016). However, the recurrence of RFP and their relationship with SAMA has not been well established (e.g., Terra-Nova et al., 2016, 2017). The direction and intensity field observed at centennial scale are not reproduced by a single mechanism (e.g., Trindade et al., 2018). Therefore, a weak-field anomaly at the South Atlantic is expected to be recurrent as previously suggested (Tarduno et al., 2015; Hare et al., 2018; Trindade et al., 2018).

7. Conclusions

We present continuous and decadal results of geomagnetic secular variation and relative paleointensity data for South Brazil for the period between 4540 and 3320 cal years BP. Magnetic remanence is carried by the pseudo-single domain (PSD) or vortex magnetite and titanomagnetite. Inclination data recorded in the Lagoa dos Patos are generally lower than the values measured in Argentina and shallower than those predicted by global geomagnetic models. Relative paleointensity recorded in the Lagoa dos Patos show similar features when compared with Argentinian data or with the predictions of geomagnetic models. Discrepancy in relation to data from southern Argentina can be attributed to several factors such as the distance between locations,
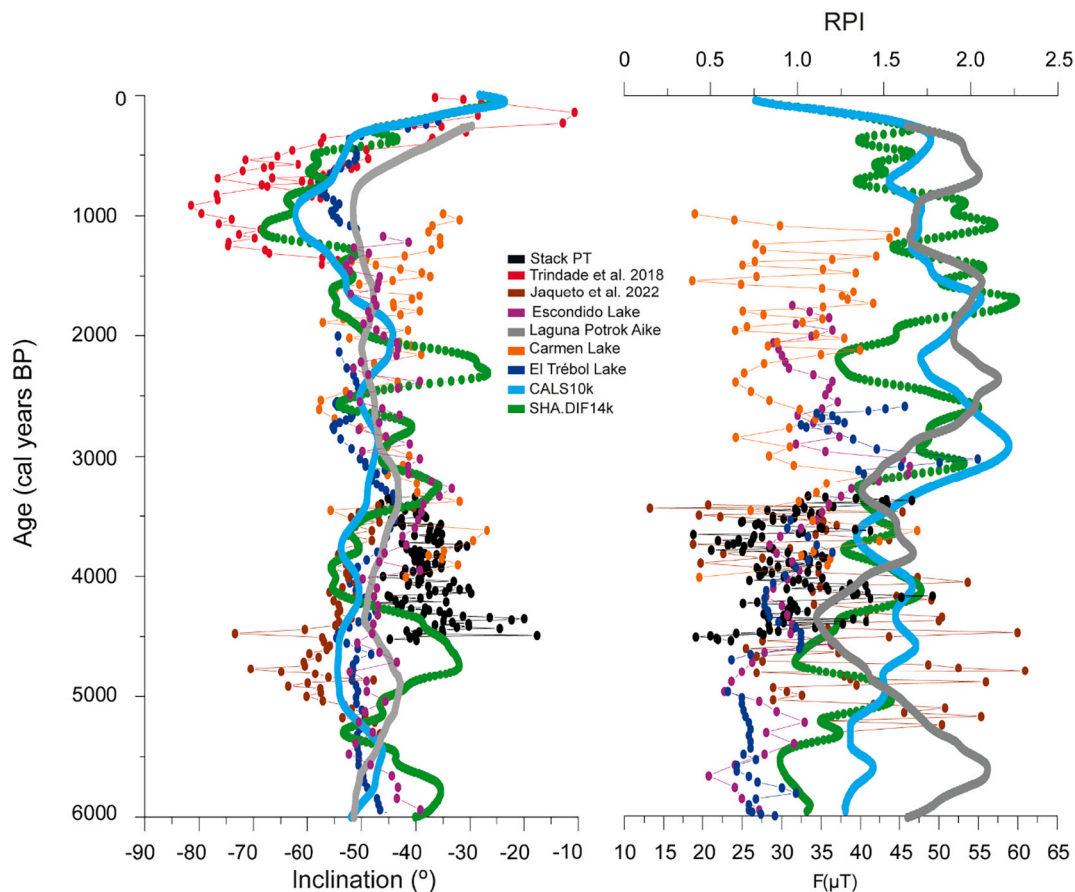
Fig. 11. a) Comparison of stacked inclination logs from Carmen Lake (Gogorza et al., 2018), Potrok Aike (Gogorza et al., 2012), El Trebol (Gogorza et al., 2006), Escondido (Gogorza et al., 2004) and Lagoa dos Patos as a function of age with the models CALS10k (Brown et al., 2015; Constable et al., 2016) and SHA.DIF.14 k (Pavón Carrasco et al., 2014) outputs. We also plotted recent data from speleothem records for that same region (Trindade et al., 2018 and Jaqueto et al., 2022). And b) comparison of normalized intensity record from Lagoa dos Patos with Carmen Lake (Gogorza et al., 2018) and with relative paleointensity records from Laguna Potrok Aike (Gogorza et al., 2012), Escondido Lake (Gogorza et al., 2004), El Trébol Lake (Gogorza et al., 2006) and the models SHA.DIF14k (Pavón-Carrasco et al., 2014) and CALS10k.2 (Brown et al., 2015; Constable et al., 2016). We also plotted recent data from speleothem records for that same region (Trindade et al., 2018 and Jaqueto et al., 2022). The lower x scale is referring to absolute paleointensity data while the upper scale is referring to relative paleointensity data. (For interpretation of the references to colour in this figure legend, the reader is referred to the web version of this article.)

differences between sampling resolution, and some local effects from non-dipole fields. On the other hand, differences between Lagoa dos Patos data and global geomagnetic field models are mainly affected by the absence of data from South Brazil. Our data contribute with more accurate geomagnetic field reconstruction for this region.

Author contributions

Camila T. Lopes: Conceptualization, Data curation, Formal analysis, Investigation, Methodology,Validation, Writing - original draft, Writing - review & editing.

Jairo F. Savian: Conceptualization, Data curation, Formal analysis, Funding acquisition, Investigation, Methodology, Project administration, Supervision, Validation.

Everton Frigo: Conceptualization, Data curation, Formal analysis, Investigation, Methodology, Supervision, Validation.

Gabriel Endrizzi: Formal analysis, Methodology.

Gelvam A. Hartmann: Conceptualization, Formal analysis, Investigation, Methodology, Validation.

Nicolau O. Santos: Data curation, Formal analysis, Methodology.

Ricardo I. F. Trindade: Conceptualization, Investigation, Methodology, Validation.

Michel D. Ivanoff: Data curation, Formal analysis, Investigation, Methodology.

Elirio E. Toldo Jr.: Conceptualization, Data curation, Formal analysis, Funding acquisition, Investigation, Methodology, Project administration, Validation.

Gerson Fauth:Data curation, Formal analysis, Investigation, Methodolog.

Lucas V. Oliveira: Data curation, Formal analysis, Investigation, Methodolog.

Marlone H. H. Bom: Data curation, Formal analysis, Investigation, Methodolog.

Declaration of Competing Interest

The authors declare that they have no known competing financial interests or personal relationships that could have appeared to influence the work reported in this paper.

Acknowledgements

Appendix A. Supplementary data

Supplementary data to this article can be found online at https://doi. org/10.1016/j.pepi.2022.106935.

References

Amit, H., Korte, M., Aubert, J., Constable, C.G., Hulot, G., 2011. The time-dependence of intense archeomagnetic flux patches. J. Geophys. Res. 116, B12106.

Banerjee, S.K., King, J., Marvin, J., 1981. A rapid method for magnetic granulometry with applications to environmental studies. Geophys. Res. Lett. 8, 333–336.

Barletta, F., St-Onge, G., Channell, J.E.T., Rochon, A., Polyak, L., Darby, D.A., 2008. High resolution paleomagnetic secular variation and relative paleointensity records from the western Canadian Arctic: implication for Holocene stratigraphy and geomagnetic field behaviour. Can. J. Earth Sci. 45, 1265–1281.

Blaauw, M., Christen, J.A., 2011. Flexible paleoclimate age-depth models using an autoregressive gamma process. Bayesian Anal. 6, 457–474.

Bloemendal, J., Lamb, B., King, J., 1988. Paleoenvironmental implications of rock-magnetic properties of late Quaternary sediment cores from the eastern equatorial Atlantic. Paleoceanography 3, 61–87.

Bloemendal, J., King, J.W., Hall, F.R., Doh, S.-J., 1992. Rock magnetism of late Neogene and Pleistocene deep-sea sediments: relationship to sediment source, diagenetic processes, and sediment lithology. J. Geophys. Res. 97, 4361–4375. https://doi.org/ 10.1029/91JB03068.

Bortolin, E.C., Weschenfelder, J., Cooper, A., 2018. Incised valley paleoenvironments interpreted by seismic stratigraphic approach in Patos Lagoon, Southern Brazil. Braz. J. Geol. 48 (3), 533–551.

Brachfeld, S., Banerjee, S.K., 2000. A new high-resolution geomagnetic paleointensity record for the north American Holocene: a comparison of sediments and absolute intensity data. J. Geophys. Res. 105 (B1), 821 e 834.

Brachfeld, S., Acton, G.D., Guyodo, Y., Banerjee, S.K., 2000. High-resolution paleomagnetic records from the Palmer deep, western Antarctic peninsula. Earth Planet. Sci. Lett. 181, 429–441.

Brown, M.C., Donadini, F., Nilsson, A., Panovska, S., Frank, U., Korhonen, K., Schuberth, M., Korte, M., Constable, C.G., 2015. GEOMAGIA50.v3: 2. A new paleomagnetic database for lake and marine sediments. Earth Planets Space 67. https://doi.org/10.1186/s40623-015-0233-z.

Channell, J.E.T., Vázquez Riveiros, N., Gottschalk, J., Waelbroeck, C., Skinner, L.C., 2017. Age and duration of Laschamp and Iceland Basin geomagnetic excursions in the South Atlantic Ocean. Quat. Sci. Rev. 167, 1–13.

Christensen, U.R., Aubert, J., Hulot, G., 2010. Conditions for earth-like geodynamo models. Earth Planet. Sci. Lett. 296, 487–496.

Collins, L.G., Hounslow, M.W., Allen, C.S., Hodgson, D.A., Pike, J., Karloukovski, V.V., 2012. Paleomagnetic and biostratigraphic dating of marine sediments from the Scotia Sea, Antarctica: first identification of the Laschamp excursion in the Southern Ocean. Quat. Geochronol. 7, 67–75.

Constable, C., Korte, M., Panovska, S., 2016. Persistent high paleosecular variation activity in southern hemisphere for at least 10 000 years. Earth Planet. Sci. Lett. 453, 78–86.

Day, R., Fuller, M., Schmidt, V.A., 1977. Hysteresis properties of titanomagnetites: grain size and composition dependence. Phys. Earth Planet. Inter. 13, 260–266.

Donadini, F., Korte, M., Constable, C.G., 2009. Geomagnetic field for 0–3 Ka: 1. New data sets for global modeling. Geochem. Geophys. Geosyst 10.

Dumberry, M., Finlay, C.C., 2007. Eastward and westward of the Earth's magnetic field for the last three millennia. Earth Planet. Sci. Lett. 254, 146–157.

Dunlop, D.J., 2002. Theory and application of the Day plot (Mrs/Ms versus Hcr/Hc) 1. Theoretical curves and tests using titanomagnetite data. J. Geophys. Res. 107 (B3), 2056.

Gallet, Y., Genevey, A., Courtillot, V., 2003. On the possible occurrence of 'archaeomagnetic jerk' in the geomagnetic field over the past three millennia. Earth Planet. Sci. Lett. 214, 237–242.

Gallet, Y., Hulot, G., Chulliat, A., Genevey, A., 2009. Geomagnetic field hemispheric asymmetry and archeomagnetic jerks. Earth Planet. Sci. Lett. 284, 179–186.

Genevey, A., Gallet, Y., Constable, C., Korte, M., Hulot, G., 2008. ArcheoInt: an upgraded compilation of geomagnetic field intensity data for the past ten millennia and its application to the recovery of the past dipole moment. Geochem. Geophys. Geosyst. 9, Q04038.

Gogorza, C.S., Sinito, A., Vilas, J., Creer, K., Nuñez, H., 2000a. Geomagnetic secular variations over the last 6500 years as recorded by sediments from the lakes of South Argentina. Geophys. J. Int. 143, 787–798.

Gogorza, C.S., Sinito, A.M., Di Tommaso, I., Vilas, J.F., Creer, K.M., Nuñez, H., 2000b. Geomagnetic secular variations 0-12 kyr as recorded by sediments from Lake Moreno (southern Argentina). J. South Am. Earth Sc. 13, 627–645.

Gogorza, C.S.G., Sinito, A.M., Di Tomasso, I., Vilas, J.F., Creer, K.M., Nunez, H., 1999. Holocene secular variation recorded by sediments from Lake Escondido (South Argentina). Earth Planets Space 51, 93–106.

Gogorza, C.S.G., Sinito, A.M., Lirio, J.M., Nuñez, H., Chaparro, M., Vilas, J.F., 2002. Paleosecular variations 0-19,000 years recorded by sediments from Escondido Lake (Argentina). Phys. Earth Planet. Int 133, 35–55.

Gogorza, C.S.G., Lirio, J.M., Nuñez, H., Chaparro, M.A.E., Bertorello, H.R., Sinito, A.M., 2004. Paleointensity studies on Holocene-Pleistocene sediments from Lake Escondido, Argentina. Phys. Earth Planet. Int. 145, 219–238.

Gogorza, C.S.G., Irurzun, M.A., Chaparro, M.A.E., Lirio, J.M., Nuñez, H., Bercoff, P.G., Sinito, A.M., 2006. Relative paleointensity of the geomagnetic field over the last 21,000 years BP from sediment cores, Lake El Trébol (Patagonia, Argentina). Earth Planets Space 58, 1323–1332.

Gogorza, C.S.G., Torcida, S., Irurzun, M.A., Chaparro, M.A.E., Sinito, A.M., Sinito, 2008. A pseudo-Thellier relative paleointensity record during the last 18,000 years from Lake El Trébol (Patagonia, Argentina). Geofis. Int. 47 (4), 319–327.

Gogorza, C.S.G., Sinito, A.M., Ohlendorf, C., Kastner, S., Zolitschka, B., 2011. Paleosecular variation and paleointensity records for the last millennium from southern South America (Laguna Potrok Aike, Santa Cruz, Argentina). Phys. Earth Planet. Int. 184, 41–50.

Gogorza, C.S.G., Irurzun, M.A., Sinito, A.M., Lisé-Pronovost, A., St-Onge, G., Haberzettl, T., Ohlendorf, C., Kastner, S., Zolitschka, B., 2012. High-resolution paleomagnetic records from Laguna Potrok Aike (Patagonia, Argentina) for the last 16,000 years. Geochem. Geophys. Geosyst. 13, 12.

Gogorza, C.S.G., Irurzun, M.A., Orgeira, M.J., Palermo, P., Llera, M., 2018. A continuous Late Holocene paleosecular variation record from Carmen Lake (Tierra del Fuego, Argentina). Phys. Earth Planet. Int. 280, 40–52.

Guyodo, Y., Valet, J.P., 1996. Relative variations in geomagnetic intensity from sedimentary records over the past 200,000 years. Earth Planet. Sci. Lett. 143, 23–26.

Hare, V.J., Tarduno, J.A., Huffman, T., Watkeys, M., Thebe, P.C., Manyanga, M., Bono, R. K., Cottrell, R.D., 2018. New archeomagnetic directional records from Iron age southern Africa (ca. 425–1550 CE) and implications for the South Atlantic anomaly. Geophys. Res. Lett. 45, 1361–1369. https://doi.org/10.1002/2017GL076007.

Hartmann, G., Genevey, A., Gallet, Y., Trindade, R., Etchevarne, C., Le Goff, M., Afonso, M.C., 2010. Archeointensity in Northeast Brazil over the past five centuries. Earth Planet. Sci. Lett. 296, 340–352.

Hartmann, G., Genevey, A., Gallet, Y., Trindade, R., Le Goff, M., 2011. New historical archeointensity data from Brazil: evidence for a large regional non-dipole field contribution over the past few centuries. Earth Planet. Sci. Lett. 306, 66–77.

Hartmann, G., Poletti, W., Trindade, R., Ferreira, L.M., Sanches, P.L.M., 2019. New archeointensity data from South Brazil and the influence of the South Atlantic anomaly in South America. Earth Planet. Sci. Lett. 512, 124–133.

Hartmann, G.A., Pacca, I.G., 2009. Time evolution of the South Atlantic magnetic anomaly. An. Acad. Bras. Ciênc. 81, 243–255.

Hellio, G., Gillet, N., 2018. Time-correlation-based regression of the geomagnetic field from archeological and sediment records. Geophys. J. Int. 214 (3), 1585–1607.

Hogg, A., Heaton, T., Hua, Q., Palmer, J., Turney, C., Southon, J., Bayliss, A., Blackwell, P.G., Boswijk, G., Ramsey, C.B., Pearson, C., Petchey, F., Reimer, P., Reimer, R., Wacker, L., 2020. SHCal20 southern hemisphere calibration, 0–55,000 years cal BP. Radiocarbon 62 (4), 759–778.

Irurzun, M.A., Gogorza, C.S.G., Sinito, A.M., Lirio, J.M., Nuñez, H., Chaparro, M.A.E., 2006. Paleosecular variations recorded by sediments from Lake El Trébol, Argentina. Phys. Earth Planet. Int. 154, 1–17.

Irurzun, M.A., Gogorza, C.S.G., Sinito, A.M., Chaparro, M.A.E., Nuñez, H., Lirio, J.M., 2008. Paleosecular variations 12–20 kyr as recorded by sediments from Lake Moreno (southern Argentina). Stud. Geophys. Geod. 52, 157–172. https://doi.org/10.1007/ s11200-008-0011-5.

Irurzun, M.A., Gogorza, C.S., Torcida, S., Lírio, J.M., Nuñez, H., Bercoff, P.G., et al., 2009. Rock magnetic properties and relative paleointensity stack between 13 and 24 kyr. Phys. Earth Planet. Inter. 172, 157–168.

Jaqueto, P., Trindade, R.I.F., Terra-Nova, F., Feinberg, J.M., Novello, V.F., Strikís, N.M., et al., 2022. Stalagmite paleomagnetic record of a quiet mid-to-late Holocene field activity in Central South America. Nat. Commun. 13, 1349.

Kaiser, J., Lamy, F., Hebbeln, D., 2005. A 70-kyr sea surface temperature record off southern Chile (ocean drilling program site 1233). Paleoceanography 20, PA4009.

King, J.W., Banerjee, S.K., Marvin, J., Ozdemir, O., 1982. A comparison of different magnetic methods for determining the relative grain size of magnetite in natural materials: some results from lake sediments, earth planet. Sci. Lett. 59, 404–419.

King, J.W., Banerjee, S.K., Marvin, J., 1983. A new rock magnetic approach to selecting sediments for geomagnetic paleointensity studies: application to paleointensity for the last 4000 years. J. Geophys. Res. 88, 5911–5921.

Kirschvink, J.L., 1980. The least-squares line and plane and the analysis of paleomagnetic data. Geophys. J. Int. 62, 699–718.

Korte, M., Constable, C., 2011. Improving geomagnetic field reconstructions for 0–3ka. Phys. Earth Planet. Int. 188, 247–259.

Korte, M., Genevey, A., Constable, C.G., Frank, U., Schnepp, E., 2005. Continuous geomagnetic field models for the past 7 millennia: 1. A new global data compilation. Geochem. Geophys. Geosyst. 6, Q02H15.

Korte, M., Donadini, F., Constable, C.G., 2009. Geomagnetic field for 0–3 ka: 2. A new series of time-varying global models. Geochem. Geophys. Geosyst. 10, Q06008.

Korte, M., Constable, C., Donadini, F., Holme, R., 2011. Reconstructing the Holocene geomagnetic field. Earth Planet. Sci. Lett. 312, 497–505.

Korte, M., Brown, M.C., Gunnarson, S.R., Nilsson, A., Panovska, S., Wardinski, I., Constable, C.G., 2019. Refining Holocene geochronologies using palaeomagnetic records. Quat. Geochronol. 50, 47–74. https://doi.org/10.1016/j.quageo.2018.11.004.

Laj, C., Kissel, C., Beer, J., 2004. High resolution global paleointensity stack since 75 kyrs (GLOPIS-75) calibrated to absolute values. In: Channell, J.E.T., Kent, D.V., Lowrie, W., Meert, J.G. (Eds.), Timescales of the Geomagnetic Field (AGU Monogr. Ser. vol. 145). American Geophysical Union, Washington, DC, pp. 255–265.

Levi, S., Banerjee, S.K., 1976. On the possibility of obtaining relative paleointensities from ake sediments. Earth Planet. Sci. Lett. 29, 219–226.

Lisé-Pronovost, A., St-Onge, G., Gogorza, C., Haberzettl, T., Preda, M., Kliem, P., Francus, P., Zolitschka, B., 2013. High-resolution paleomagnetic secular variations and relative paleointensity since the Late Pleistocene in southern South America. Quat. Sci. Rev. 71, 91–108.

Liu, Q.S., Roberts, A.P., Torrent, J., Horng, C.S., Larrasoaña, J.C., 2007. What do the HIRM and S-ratio really measure in environmental magnetism? Geochem. Geophys. Geosyst. 8, Q09011. https://doi.org/10.1029/2007GC001717.

2006b. Late Quaternary paleomagnetic secular variation and chronostratigraphy from ODP sites 1233 and 1234. In: Lund, S.P., Stoner, J., Lamy, F., Tiedemann, R., Mix, A. C., Richter, C., Ruddiman, W.F. (Eds.), 2006. Proceedings of the Ocean Drilling Program, Scientific Results, 202.

Macri, P., Sagnotti, L., Dinares-Turell, J., Caburlotto, A., 2005. A composite record of Late Pleistocene relative geomagnetic paleointensity from the Wilkes Land Basin (Antarctica). Phys. Earth Planet. Int. 151, 223–242.

Macrì, P., Sagnotti, L., Dinarès-Turell, J., Caburlotto, A., 2010. Relative geomagnetic paleointensity of the Brunhes Chron and the Matuyama-Brunhes precursor as recorded in sediment core from Wilkes Land Basin (Antarctica). Phys. Earth Planet. Int. 179, 72–86.

Martins, I.R., Villwock, J.A., Martins, L.R., Benvenuti, C.E., 1989. The Lagoa dos Patos Estuarine Ecosystem. Pesquisas 22, 5–44.

Mazaud, A., Sicre, M.A., Ezat, U., Pichon, J.J., Duprat, J., Laj, C., Kissel, C., Beaufort, L., Michel, E., Turon, J.L., 2002. Geomagnetic-assisted stratigraphy and sea surface temperature changes in core MD94-103 (southern Indian Ocean): possible implications for north-south climatic relationships around H4. Earth planet. Sci. Lett. 201 (1), 15, 159–170.

Muscheler, R., Adolphi, F., Knudsen, M.F., 2014. Assessing the differences between the IntCal and Greenland ice-core time scales for the last 14,000 years via the common cosmogenic radionuclide variations. Quat. Sci. Rev. 106, 81–87.

Nilsson, A., Snowball, I., Muscheler, R., 2010. Holocene geocentric dipole tilt model constrained by sedimentary paleomagnetic data. Geochem. Geophys. Geosyst. 11, Q08018.

Nilsson, A., Muscheler, R., Snowball, I., Aldahan, A., Possnert, G., Augustinus, P., Atkin, D., Stephens, T., 2011. Multi-proxy identification of the Laschamp geomagnetic field excursion in Lake Pupuke, New Zealand. Earth Planet. Sci. Lett. 311 (1–2), 155–164.

Nilsson, A., Holme, R., Korte, M., Suttie, N., Hill, M., 2014. Reconstructing Holocene geomagnetic field variation: new methods, models and implications. Geophys. J. Int. 198 (1), 229–248.

Olson, P., Amit, H., 2006. Changes in earth's dipole. Naturwissenschaften 93 (11), 519–542.

Panovska, S., Constable, C., Brown, M., 2018. Global and regional assessments of paleosecular variation activity over the past 100 ka. Geochem. Geophys. Geosyst. 19 (5), 1559–1580.

Panovska, S., Korte, M., Constable, C.G., 2019. One hundred thousand years of geomagnetic field evolution. Rev. Geophys. 57, 1289–1337.

Pavón Carrasco, F.J., Rodríguez-González, J., Osete, M.L., Torta, J.M., 2014. A Matlab tool for archaeomagnetic dating. J. Archaeol. Sci. 38, 408–419.

Peters, C., Dekkers, M.J., 2003. Selected room temperature magnetic parameters as a function of mineralogy, concentration and grain size. Phys. Chem. Earth 28, 659–667. https://doi.org/10.1016/S1474-7065(03)00120-7.

Poletti, W., Trindade, R.I., Hartmann, G.A., Damiani, N., Rech, R.M., 2016. Archaeomagnetism of Jesuit missions in South Brazil (1657–1706 AD) and assessment of the south American database. Earth Planet. Sci. Lett. 445, 36–47.

Roberts, A.P., Winklhofer, M., 2004. Why are geomagnetic excursions not always recorded in sediments? Constrains from post-depositional remanent magnetization lock-in modelling. Earth Planet. Sci. Lett. 227, 345–359.

Roberts, A.P., Cui, Y.L., Verosub, K.L., 1995. Wasp-waisted hysteresis loops: mineral magnetic characteristics and discrimination of components in mixed magnetic system. J. Geophys. Res. 100, 17909–17924.

Roberts, A.P., Tauxe, L., Heslop, D., Zhao, X., Jiang, Z., 2018. A critical appraisal of the "Day" diagram. J. Geophys. Res. Solid Earth 123, 2618–2644.

Snowball, I., Sandgren, P., 2004. Geomagnetic field intensity changes in Sweden between 9000 and 450 cal BP: extending the record of "archaeomagnetic jerks" by means of

lake sediments and the pseudo-Thellier technique. Earth Planet. Sci. Lett. 227, 361–376.

Stoner, J.S., St-Onge, G., 2007. Magnetic stratigraphy in paleoceanography: Reversals, excursions, paleointensity, and secular variation. In: Hillaire-Marcel, C., deVernal, A. (Eds.), Proxies in Late Cenozoic Paleoceanography, Dev. In Mar. Geol., Vol. 1. Elsevier, Amsterdam, pp. 99–138. https://doi.org/10.1016/S1572-5480(07)01008-1.

Stoner, J.S., Laj, C., Channell, J.E.T., Kissel, C., 2002. South Atlantic and North Atlantic geomagnetic paleointensity stacks (0-80 ka): implications for interhemispheric correlation. Quat. Sci. Rev. 21, 1141–1151.

Stoner, J.S., Channell, J.E.T., Hodell, D.A., Charles, C.D., 2003. A 580 kyr paleomagnetic record from the sub-Antarctic South Atlantic (ocean drilling program site 1089). J. Geophys. Res. 108 (B5), 2244.

Suganuma, Y., Yokoyama, Y., Yamazaki, T., Kawamura, K., Horng, C.S., Matsuzaki, H., 2010. 10Be evidence for delayed acquisition of remanent magnetization in marine sediments: implication for a new age for the Matuyama-Brunhes boundary. Earth Planet. Sci. Lett. 296, 443–450.

Suganuma, Y., Okuno, J., Heslop, D., Roberts, A.P., Yamazaki, T., Yokoyama, Y., 2011. Post-depositional remanent magnetization lock-in for marine sediments deduced from 10Be and paleomagnetic records through the Matuyama-Brunhes boundary. Earth Planet. Sci. Lett. 311, 39–52.

Tarduno, J., Watkeys, M., Huffman, T., Cottrell, R.D., Blackman, E.G., Wendt, A., Scribner, C.A., Wagner, C.L., 2015. Antiquity of the South Atlantic anomaly and evidence for top-down control on the geodynamo. Nat. Commun. 6, 7865. https://doi.org/10.1038/ncomms8865.

Tauxe, L., 1993. Sedimentary records of relative paleointensities of the geomagnetic field: theory and practice. Rev. Geophys. 31, 319–354.

Tauxe, L., 2005. Inclination flattening and the geocentric axial dipole hypothesis. Earth Planet. Sci. Lett. 233, 247–261.

Tauxe, L., Pick, T., Kok, Y.S., 1995. Relative paleointensity in sediments: A Pseudo-Thellier approach. Geophys. Res. Lett. 22, 2885–2888. https://doi.org/10.1029/95GL03166.

Tauxe, L., Mullender, T.A.T., Pick, T., 1996. Potbellies, wasp-waists, and superparamagnetism in magnetic hysteresis. J. Geophys. Res. 101 (B1), 571–583.

Tauxe, L., Kodama, K.P., Kent, D.V., 2008. Testing corrections for paleomagnetic inclination error in sedimentary rocks: A comparative approach. Phys. Earth Planet. Inter. 169, 152–165.

Terra-Nova, F., Amit, H., Hartmann, G.A., Trindade, R.I.F., 2015. The time dependence of reversed archeomagnetic flux patches. J. Geophys. Rese. Solid Earth 120, 691–704.

Terra-Nova, F., Amit, H., Hartmann, G.A., Trindade, R.I.F., 2016. Using archaeomagnetic field models to constrain the physics of the core: robustness and preferred locations of reversed flux patches. Journal of Geophysical International 206, 1890–1913.

Terra-Nova, F., Amit, H., Hartmann, G.A., Trindade, R.I.F., Pinheiro, K.J., 2017. Relating the South Atlantic anomaly and geomagnetic flux patches. Phys. Earth Planet. Inter. 266, 39–53.

Thompson, R., Oldfield, F., 1986. Environmental Magnetism. Allen & Unwin Ltd, p. 225.

Toldo Jr., E.E., 1989. Os Efeitos do Transporte Sedimentar na Distribuição dos Tamanhos de Grão e Morfodinâmica da Lagoa dos Patos. Mestrado em Geociências. Programa de Pós-Graduação em Geociências. Universidade Federal do Rio Grande do Sul, p. 143p.

Toldo Jr., E.E., Dillenburg, S.R., Corrêa, I.C.S., Almeida, L.E.S.B., 2000. Holocene sedimentation in Lagoa dos Patos lagoon, Rio Grande do Sul, Brazil. J. Coast. Res. 16, 816–822.

Toldo Jr., E.E., Almeida, L.E.S.B., Corrêa, I.C.S., 2003. Forecasting shoreline changes of Lagoa dos Patos lagoon, Brazil. J. Coast. Res. SI35, 43–50.

Toldo Jr., E.E., Dillenburg, S.R., Corrêa, I.C.S., Almeida, L.E.S.B., Weschenfelder, J., Gruber, N.L.S., 2006. Sedimentação de Longo e Curto Período na Lagoa dos Patos, Sul do Brasil. Pesq Geos 33 (2), 79–86.

Trindade, R.I.F., Jaqueto, P., Terra-Nova, F., Brandt, D., Hartmann, G.A., Feinberg, J.M., et al., 2018. Speleothem record of geomagnetic South Atlantic anomaly recurrence. Proc. Natl. Acad. Sci. U. S. A. 115 (52) https://doi.org/10.1073/pnas.1809197115, 13,198-13,203.

Turner, G.M., Howarth, J.D., de Gelder, G.I.N.O., Fitzsimons, S.J., 2015. A new highresolution record of Holocene geomagnetic secular variation from New Zealand. Earth Planet. Sci. Lett. 430, 296–307.

Willmott, V., Domack, E.W., Canals, M., Brachfeld, S., 2006. A high resolution paleointensity record from the Gerlache-Boyd paloe-ice stream region, northern Antarctic peninsula. Quat. Res. 66, 1–11.

Yu, Y., Doh, S.-J., Kim, W., Park, Y.-H., Lee, H.-J., Yim, Y., Cho, S.-G., Oh, Y.-S., Lee, D.-S., Lee, H.-H., Gong, M.-G., Hyun, D.-H., Cho, J.-K., Sin, Y.-S., Do, M.-S., 2010. Archeomagnetic secular variation from Korea: implication for the occurrence of global archeomagnetic jerks. Earth Planet. Sci. Lett. 294, 173–181.

Zijderveld, J.D.A., 1967. AC demagnetization of rock: Analysis of results. In: Collinson, D.W., Creer, K.M., Runcorn, S.K. (Eds.), Methods in Paleomagnetism. Elsevier, Amsterdam, The Netherlands, pp. 254–286.